Mechanism-Guided Development of VO(salen)X Complexes as Catalysts for the Asymmetric Synthesis of Cyanohydrin Trimethylsilyl Ethers

Yuri N. Belokon,[b] William Clegg,[a] Ross W. Harrington,[a] Victor I. Maleev,[b] Michael North,*[a] Marta Omedes Pujol,[a] Dmitry L. Usanov,[a] and Carl Young[a]

Abstract: The mechanism by which oxovanadium(V)(salen) complexes[1] VO(salen)X catalyze the asymmetric addition of trimethylsilyl cyanide to benzaldehyde has been studied. The reaction kinetics indicated that the structure of the counterion (X) had a significant influence on the rate, but not on the enantioselectivity of the reaction. The less coordinating the counterion, the lower the catalytic activity; a trend that was confirmed by a Hammett analysis. Variable temperature kinetics allowed the enthalpies and entropies of activation to be determined for some catalysts, and showed that, for others, the overall reaction order changes from second order to zero order as the temperature is reduced. The order with respect to the catalyst was determined for nine of the VO(salen)X complexes and showed that the less active catalysts were active predominantly as mononuclear species whilst the more active catalysts were active predominantly as dinuclear species. Mass spectrometry confirmed the formation of dinuclear species in situ from all of the VO(salen)X complexes and indicated that the dinuclear complexes contained one vanadium(V) and one vanadium(IV) ion. The latter conclusion was supported by cyclic voltammetry of the complexes, by fluorescence measurements and by the fact that catalyst deactivation occurs when reactions are carried out under an inert atmosphere. Based on this evidence, it has been deduced that the catalysis involves two catalytic cycles: one for catalysis by mononuclear VO(salen)X species and the other for catalysis by dinuclear species. The catalytic cycle involving dinuclear species involves activation of both the cyanide and aldehyde, whereas the catalytic cycle involving mononuclear species activates only the aldehyde, thus explaining the higher catalytic activity observed for catalysts which are predominantly active as dinuclear complexes. Based on these mechanistic results, two new VO(salen)X complexes (X=F and NCS) were predicted to form highly active catalysts for asymmetric cyanohydrin synthesis. VO(salen)NCS was indeed found to be the most active catalyst of this type and catalyzed the asymmetric addition of trimethylsilyl cyanide to thirteen aldehydes. In each case, high yields and enantioselectivities were obtained after a reaction time of two hours at room temperature using just 0.1 mol% of the catalyst.

Keywords: aldehydes · asymmetric catalysis · cyanides · reaction mechanisms · vanadium

[a] Prof. W. Clegg, Dr. R. W. Harrington, Prof. M. North, M. O. Pujol, D. L. Usanov, C. Young
School of Chemistry and University Research Centre in Catalysis and Intensified Processing
Newcastle University
Bedson Building, Newcastle upon Tyne, NE1 7RU (UK)
Fax: (+44) 870-131-3783
E-mail: michael.north@ncl.ac.uk.

[b] Prof. Y. N. Belokon, Dr. V. I. Maleev
A.N. Nesmeyanov Institute of Organo-Element Compounds
Russian Academy of Sciences
119991, Moscow, Vavilov 28 (Russian Federation)

Supporting information for this article is available on the WWW under http://www.chemeurj.org/ or from the author.

[1] The square brackets normally used to describe complexes, such as [VO(salen)X], have been omitted in this manuscript to remove any confusion with the square brackets used for the concentration values.

Introduction

The asymmetric addition of cyanide to an aldehyde to form a non-racemic cyanohydrin is a reaction, which has been known since 1908.[1] Oxynitrilase enzymes are widespread in the plant kingdom and can be used to accomplish this reaction by using hydrogen cyanide as the cyanide source.[2] However, the enzymatic approach suffers from a number of limitations including: the need to handle hydrogen cyanide, slow reactions, limited substrate tolerance, and the availability of only one enantiomer of an enzyme. In view of these limitations and the commercial importance of enantiomerically pure α-hydroxy-acids,[3] the last ten years have seen an explosion of interest in the development of chiral Lewis acids and/or Lewis bases as catalysts for the asymmetric addition of various cyanide sources to aldehydes and ketones.[4] Currently, the most effective Lewis acids for the asymmetric

synthesis of aldehyde-derived cyanohydrins are the bimetallic titanium(salen[5]) complex **1** developed by our group,[6,7] and the aluminum(binol) complexes **2** and **3** developed by Shibasaki,[8,9] and Najera,[10] respectively. Shibasaki also developed the titanium or lanthanide complexes of glucose derived ligands **4**, as highly effective catalysts for the asymmetric synthesis of ketone-derived cyanohydrins.[9,11] Complexes **1–3** will catalyze the asymmetric addition of trimethylsilyl cyanide to aldehydes (Scheme 1) with good enantioselectivities under optimized conditions, and the use of other cyanide sources, such as cyanoformates,[12] cyanophosphonates[13] and acyl cyanides,[14] has also been achieved.
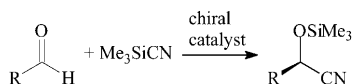
Scheme 1. Asymmetric addition of trimethylsilyl cyanide to aldehydes.
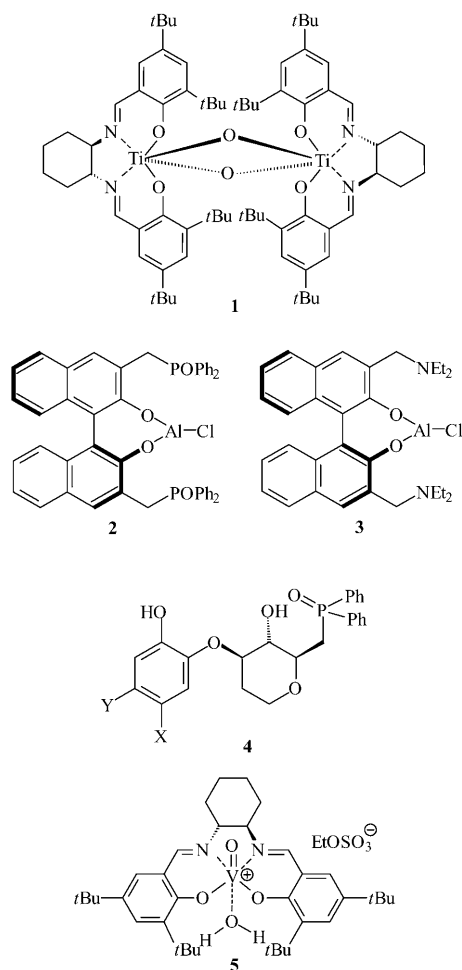
Subsequent to the development of titanium(salen) complex **1**, manganese,[15] aluminum[16] and lithium[17] salen complexes have also been found to catalyze the asymmetric addition of trimethylsilyl cyanide to aldehydes and ketones. A further significant advance was our development of oxovanadium(salen) complex **5** as the first vanadium-based catalyst for asymmetric cyanohydrin synthesis.[18] Compared to titanium complex **1**, complex **5** is a more enantioselective catalyst for the asymmetric addition of trimethylsilyl cyanide to aldehydes, but is also significantly less reactive. Nevertheless, catalyst **5** has been adopted by other research groups for use in synthesis projects.[19] In a preliminary study we reported that the catalytic activity, but not the enantioselectivity, of complexes of general structure VO(salen)X was critically dependent upon the structure of X.[20] Complexes **1** and **5** have the unique ability to utilize potassium cyanide as the cyanide source for asymmetric cyanohydrin synthesis[21] and recyclable versions of both of these catalysts have been prepared.[22]

Herein we report a detailed study of the asymmetric synthesis of cyanohydrin trimethylsilyl ethers catalyzed by VO-(salen)X complexes.[23] This study showed that catalysis can occur through mononuclear and/or binuclear species, with the latter involving both vanadium(V) and vanadium(IV) ions, and resulted in the discovery of VO(salen)NCS as the most active vanadium-based catalyst for asymmetric cyanohydrin synthesis yet developed.

Results and Discussion

Effect of counterion on catalytic activity: Complex **5** is coordinatively saturated, so our first hypothesis as to its mode of action was that dissociation of the water molecule would generate a five-coordinate Lewis-acidic metal ion which could coordinate to the aldehyde. Attack of cyanide on the activated aldehyde within the chiral coordination environment of the vanadium ion would then account for both the catalysis and enantioselectivity. To test this theory, complexes **6a–e** were prepared in the expectation that the complexes with the most strongly coordinating counterions would show the lowest catalytic activity, and that the triflate complex **6a** would exhibit enhanced catalytic activity.

6a–f

a: X = CF$_3$SO$_3$
b: X = BF$_4$
c: X = NO$_3$
d: X = Br
**e**: X = Cl
f: X = F
g: X = NCS
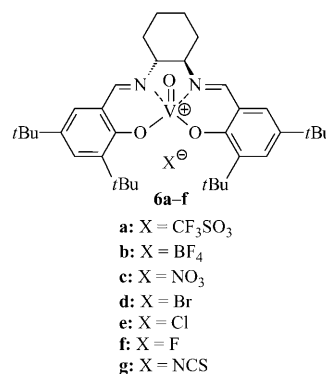
Complexes **6a–c** were prepared by ion-exchange from complex **5** on a DOWEX 1X8-400 resin. The formation of

complexes **6a,b** was readily confirmed by using ^{19}F NMR spectroscopy. Complex **6b** displays two signals in its ^{19}F NMR spectrum with relative intensities 1:3, which indicates that the tetrafluoroborate counterion is partly coordinated to the vanadium ion through one of the fluorine atoms as previously reported for an achiral VO(salen)BF$_4$ complex.[24] Complex **6c** was also prepared more conveniently by treating either complex **5** or VO(salen)[21b] with ceric ammonium nitrate,[25] and both methods gave complex **6c** with identical spectroscopic and catalytic properties. Complex **6d** was also prepared by ion-exchange on a DOWEX 1X8-400 resin, though, in this case, it was advantageous to use complex **6b** as the starting material, as the absence of a signal in the ^{19}F NMR spectrum of the product provided a convenient test for the completeness of the ion-exchange procedure. Complex **6e** was prepared by direct treatment of salen ligand **7** with vanadium oxychloride in THF, as shown in Scheme 2.
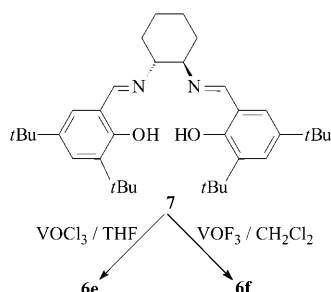
Scheme 2. Synthesis of complexes **6e** and **6f**.

The catalytic activity of each of the complexes **5** and **6a–e** was investigated by a study of the reaction kinetics for the addition of trimethylsilyl cyanide to benzaldehyde under standardized conditions ([PhCHO] = 0.49 M, [Me$_3$SiCN] = 0.56 M, [catalyst] = 9.8×10^{-4} M, dichloromethane solvent), as shown in Scheme 3. The progress of the reactions was monitored by measuring the UV absorbance (at 246 nm) of residual benzaldehyde at appropriate intervals during the reaction. At the end of the reaction, the mandelonitrile trimethylsilyl ether was converted into O-acetyl mandelonitrile by the method of Kagan[26] to allow the enantioselectivity of the silylcyanation reaction to be determined by chiral GC analysis. Reactions were first carried out at 293±0.5 K, the resulting kinetic profiles are shown in Figure 1, and the cor-
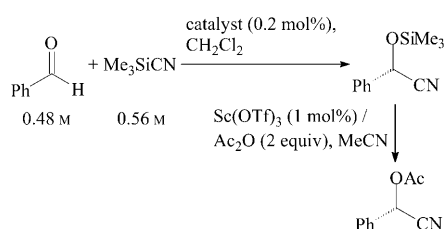
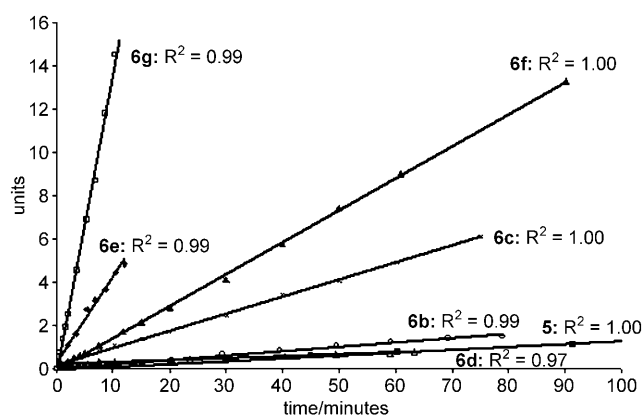Scheme 3. Reaction used to study the kinetics of asymmetric cyanohydrin synthesis.

Figure 1. Second-order kinetics plots for catalysts **5** and **6b–g** at 293 K. The reaction catalyzed by complex **5** was monitored for 150 minutes (resulting in 60% reaction). Only the first 100 minutes are shown to allow all the catalysts studied to be displayed on the same scale, but the R^2 value and the rate constant are based on all the data. The units used for the vertical scale are: $([PhCHO]_0 - [Me_3SiCN]_0)^{-1} \ln([Me_3SiCN]_0 [PhCHO]_t [Me_3SiCN]_t^{-1} [PhCHO]_0^{-1})$ in which the subscripts 0 and t refer to initial concentrations and concentrations at time t respectively.

responding apparent second-order rate constants are given in Table 1.

Table 1. Apparent second-order rate constants for complexes **5** and **6a–g** at 293 K.[a]

Complex	Counterion	$k_{2app} \times 10^4$ [M^{-1} s^{-1}]	ee [%][b]
5	EtOSO$_3^-$	2.2	91 (S)
6a	CF$_3$SO$_3^-$	0	–
6b	BF$_4^-$	3.4	90 (S)
6c	NO$_3^-$	13	95 (S)
6d	Br$^-$	1.5	94 (S)
6e	Cl$^-$	67	93 (S)
6f	F$^-$	25	91 (S)
6g	NCS$^-$	228	95 (S)

[a] Reactions carried out at 293±0.5 K under the conditions shown in Scheme 3. k_{2app} was calculated from the slopes of the second-order kinetics plots shown in Figure 1. [b] Determined by chiral GC analysis of mandelonitrile acetate.

Contrary to initial expectations, complex **6a** was found to be catalytically inactive, which immediately suggested that the Lewis acidity of the vanadium ion was not the key factor in determining the catalytic activity of the complexes. Each of the complexes **5** and **6b–e** was catalytically active and the reactions all obeyed second-order kinetics for all data points between 0 and 33–90% reaction depending on the rate of catalysis, Figure 1. The observation of second-order kinetics was unexpected, as titanium based catalyst **1** (and related complexes with modified salen ligands) had all exhibited first-order kinetics (rate = k_{1app}[Me$_3$SiCN] in which $k_{1app} = k_1$[catalyst]^x) and a catalytic cycle consistent with this kinetic behavior had been deduced.[27] The same first-order kinetics had also been observed for reactions involving other cyanide sources catalyzed by complex **1**.[12f,21b] These kinetics results indicated that asymmetric cyanohydrin syn-

thesis catalyzed by oxovanadium(salen) complexes occurred by a totally different mechanism to reactions catalyzed by titanium(salen) complexes. Experiments carried out with catalyst **6e** varying the concentrations of trimethylsilyl cyanide and benzaldehyde were only consistent with a rate equation, which was first order in both benzaldehyde and trimethylsilyl cyanide,[28] thus giving the rate equation: rate $= k_{2app}$[PhCHO][Me$_3$SiCN] in which $k_{2app} = k_2$[catalyst]^x. The value of x will vary from catalyst to catalyst and this is discussed in the following section.

Although the structure of the counterion had a major influence on the rate of addition of trimethylsilyl cyanide to benzaldehyde, it did not influence the enantioselectivity of the reaction, as in each case O-acetyl mandelonitrile with $93 \pm 3\%$ *ee* was obtained (Table 1). This indicated that the rate-determining step was not the enantiodetermining step and suggested that the counterion may not be coordinated to vanadium during the enantiodetermining step. The effect of the counterion on the apparent second-order rate constant is $Cl > NO_3 > BF_4 > EtOSO_3 > Br \gg CF_3SO_3$ and this trend suggests that the more coordinating the counterion the more reactive a catalyst will be formed. Thus, triflate is expected to be a totally non-coordinating ligand and the crystal structure of a related VO(salen) triflate complex confirmed that this was the case, with a water molecule occupying the sixth coordination site around the vanadium ion.[29] Similar literature precedent also suggested that the bromide[30] and nitrate[31] counterions would be non-coordinating, with a water molecule again occupying the sixth coordination site around the vanadium ion. In the case of bromide complex **6d** this was supported by combustion analysis results, which indicated the presence of water within the complex. The previously reported crystal structure[21b] of complex **5** also showed that the ethylsulfate counterion was not coordinated to the vanadium ion; again a water molecule occupies the sixth coordination site around the vanadium ion.

The ^{19}F NMR spectrum of complex **6b** indicated that the tetrafluoroborate counterion was present as an equilibrating mixture of coordinated and dissociated forms consistent with literature precedent[24] on a related VO(salen)BF$_4$ complex. The two crystal structures available on VO(salen)BF$_4$ complexes further support this equilibrium, as one indicates that the tetrafluoroborate anion is coordinated to the vanadium ion, whereas the other shows no coordination with the sixth coordination site of the vanadium ion being filled by a solvent molecule.[24] There are a number of reported crystal structures of vanadium(salen) complexes containing chloride units and, in contrast to the crystal structures related to complexes **5** and **6a–d**, they all contain a covalent V—Cl bond.[32]

The apparent second-order rate constants (Table 1) suggest that there may be a link between the catalytic activity of complexes **5** and **6a–e** and whether or not the counterion coordinates to the vanadium ion. The three least active complexes (**5** and **6a,d**) all have non-coordinating counterions, whereas complex **6b** which has a more coordinating coun-

terion displays higher catalytic activity, and complex **6e** with a chloride counterion known to bind covalently to vanadium shows the highest activity. The trend is further supported by the activity of complexes **6f,g** as discussed later.

However, other factors must also be involved in determining the catalytic activity, as tetrafluoroborate complex **6b** has lower catalytic activity than would be expected and the wide range of catalytic activities exhibited by complexes **5** and **6a,c,d**, all of which are expected to have non-coordinating counterions with a water molecule coordinated to the vanadium ion, is not accounted for by this simple analysis. Trimethylsilyl cyanide is a good silylating agent,[33] so the coordinated water molecule present in complexes **5** and **6a,c,d** is likely to be converted into non-coordinating bis-trimethylsilyl ether during a cyanosilylation reaction. Another factor which could affect the apparent rate constants is the order with respect to the catalyst ($k_{2app} = k_2$[catalyst]^x), since our previous work on the use of complex **1** and related titanium-(salen) complexes showed that this is determined by the number of metal(salen) units involved in the catalytic cycle and the equilibrium constant(s) between these species.[27a] Thus it was expected that x would vary from catalyst to catalyst and influence the relative reactivities of the complexes.

Determination of order with respect to catalyst: As $k_{2app} = k_2$[catalyst]^x, a plot of $\ln(k_{2app})$ against $\ln$[catalyst] should have gradient x, thus allowing the order with respect to the catalyst to be determined from reactions carried out at different catalyst concentrations. This analysis was carried out for each of catalysts **5** and **6b–e**, as shown in Figure 2,[28] and
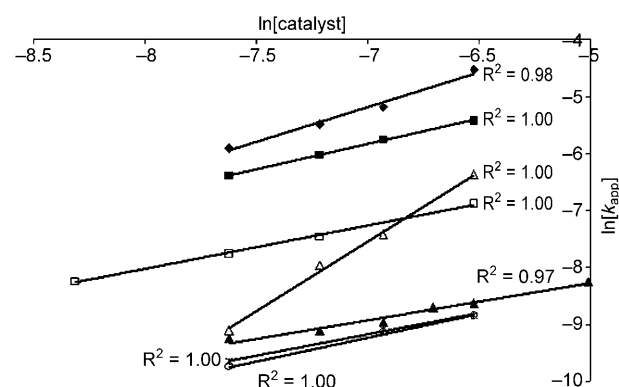

Figure 2. Plots of $\ln(k_{app})$ against $\ln$[catalyst] for complexes **5** and **6b–e,g** at 273 K. **5**: ▲, **6b**: ○, **6c**: □, **6d**: ✳, **6e**: ■, **6f**: △, **6g**: ◆.

the resulting orders with respect to the catalyst are given in Table 2. The orders with respect to the catalyst can be used to provide information on the number of VO(salen) units involved in the catalytic cycle and on the oligomeric nature of the catalytically active species, as previously described for titanium-based catalysts.[27a] There are four limiting cases. If the complex is catalytically active as a mononuclear species, then:

Table 2. Reaction orders with respect to the catalyst for complexes **5** and **6b–g**.

Catalyst	Reaction order (x) with respect to catalyst
1	1.34[a]
5	0.64
6b	0.84
6c	0.77
6d	0.74
6e	0.88
6f	2.45
6g	1.23

[a] Value taken from reference [27a].

i)   if the mononuclear complex is the predominant species present in solution: rate $= k$[catalyst]^1

ii) if a dinuclear complex is the predominant species present in solution: rate $= k$[catalyst]$^{0.5}$

If the complex is catalytically active as a dinuclear species, then:

iii) if the mononuclear complex is the predominant species present in solution: rate $= k$[catalyst]^2

iv) if a dinuclear complex is the predominant species present in solution: rate $= k$[catalyst]^1

For titanium-based catalysts, the order with respect to the catalyst is always > 1, thus indicating that the catalysts are always catalytically active as dinuclear species.[27a] However, as the data in Table 2 show, the vanadium-based complexes exhibit more variability. For complexes **5** and **6b–e** the order with respect to the catalyst is between 0.6 and 0.9, which suggests that the predominant catalytically active species is mononuclear, though this is in equilibrium with dinuclear species, which may also have some catalytic activity.

These results confirmed that the mechanism of catalysis using VO(salen)X complexes was fundamentally different to the mechanism by, which titanium-based catalyst **1** catalyzes the same reaction. The simplest explanation of the observed orders with respect to the catalyst is that, for all of the VO-(salen)X complexes, both mononuclear and binuclear complexes are present in the reaction mixture and both are catalytically active. The counterion influences the equilibrium between, and/or relative catalytic activity of, the mononuclear and dinuclear complexes.

Mass spectra of VO(salen)X complexes: The high-resolution, positive-ion mode electrospray mass spectra of each of complexes **5** and **6a–e** were obtained from a 1:1 dichloromethane/methanol solution of the complex.[28] In all cases, an ion cluster corresponding to a species containing a single vanadium ion was observed with a base peak at m/z 611. Both the high-resolution masses and the isotope distribution indicate that this corresponds to the expected [VO(salen)]$^+$ ion. However, in all cases the spectra also showed a second ion cluster with a base peak at m/z 1222. The isotope pattern

for this peak indicates the presence of two vanadium ions, and the high-resolution masses indicate that it corresponds to the [VO(salen)]$_2$$^+$ ion. Importantly, this is a monocharged ion obtained from two vanadium(V) units, so one of the two vanadium ions must have been reduced to vanadium(IV) within the mass spectrometer (the ^{1}H NMR spectra of the complexes showed no evidence of the presence of paramagnetic vanadium(IV) species). No evidence for the formation of [VO(salen)]$_2$$^{2+}$ was observed in any of the mass spectra (this ion would appear at m/z 611, but the individual lines within the isotope pattern would be separated by only 0.5 m/z units, allowing it to be easily distinguished from [VO(salen)]$^+$).

Vanadium(V)(salen) complexes are well known oxidizing agents,[25,34,35,36] so the formation of vanadium(IV)(salen) units can be explained by oxidation of the methanol solvent. The ratio of monuclear to dinuclear species varied from complex to complex (between 2:1 and 16:1), but this will be sensitive to the time between preparation of the solution and recording the spectra as well as the structure of the counterion. Nevertheless, the mass spectrometry results did support the results of the catalyst order determinations by showing that complexes **5** and **6a–e** can form both monuclear and dinuclear species in solution and indicated that the dinuclear species would be derived from one vanadium(V) and one vanadium(IV) ion.[37]

Effect of temperature on catalytic activity: To determine the thermodynamic origin of the influence of the counterion on the catalytic activity of the complexes, the catalytic activity of selected complexes was studied at various temperatures to allow the enthalpies and entropies of activation of the complexes to be determined. Complex **6a** was also found to be catalytically inactive at 273 K. For comparison purposes titanium(salen) complex **1** was also included in this study, as the temperature dependence of its catalytic activity had not previously been investigated. Reactions could be monitored only over a temperature range of 263 K to 298 K as above 298 K the volatility of the dichloromethane solvent was found to reduce the accuracy of the results. Below 263 K, significant reaction was found to occur in the microlitre syringe used to withdraw samples for analysis, thus preventing reliable analysis of the extent of reaction. The results obtained are shown in Table 3.[28]

The most surprising result of this variable-temperature study was that for some, but not all, of catalysts **5** and **6b–e** the apparent reaction order changed from second order to zero order, as the temperature was reduced from 293 K to 263 K, corresponding to a change in the rate equation from rate $= k_{2app}$[PhCHO][Me$_3$SiCN] to rate $= k_{0app}$ in which $k_{0app} = k_0$[catalyst]^x. Thus, although catalysts **5** and **6e** displayed second-order kinetics at all temperatures studied, catalysts **6b–d** displayed zero-order kinetics at 263 K and at some of the intermediate temperatures. In the case of catalyst **6c**, the change from zero- to second-order kinetics occurs over a narrow temperature range as the kinetic data fit only zero-order kinetics at 263 K, but fit only second-

Table 3. Reaction order and rate constants for complexes **5**, and **6b–e,g** at various temperatures.[a,b]

| Complex | Reaction order (apparent rate constant ×10⁴) | | | |
	263 K	273 K	283 K	293 K
1	1 (12 s⁻¹)	1 (25 s⁻¹)	1 (40 s⁻¹)	1 (75 s⁻¹)
6b	0 (0.6 M s⁻¹)	0 (0.5 M s⁻¹)	0 (0.6 M s⁻¹)	2 (3.4 M⁻¹ s⁻¹)
6c	0 (0.7 M s⁻¹)	2 (9.4 M⁻¹ s⁻¹)	–	2 (13 M⁻¹ s⁻¹)
6d	0 (0.7 M s⁻¹)	0 (1.1 M s⁻¹)	2 (1.5 M⁻¹ s⁻¹)	2 (1.5 M⁻¹ s⁻¹)
6e	2 (13 M⁻¹ s⁻¹)	2 (26 M⁻¹ s⁻¹)	2 (40 M⁻¹ s⁻¹)	2 (67 M⁻¹ s⁻¹)
6f	2 (3.9 M⁻¹ s⁻¹)	2 (6 M⁻¹ s⁻¹)	2 (12 M⁻¹ s⁻¹)	2 (24 M⁻¹ s⁻¹)
6g	2 (80 M⁻¹ s⁻¹)	2 (105 M⁻¹ s⁻¹)	–	2 (228 M⁻¹ s⁻¹)

[a] Reactions carried out at the specified temperature ±0.5°C under the conditions shown in Scheme 3. Apparent rate constants were calculated from the slopes of the appropriate kinetics plots. [b] Reactions with complex **5** were carried out at 278 K (k_{2app} = 1.1 M s⁻¹), 288 K (k_{2app} = 1.6 M s⁻¹), 293 K (k_{2app} = 2.2 M s⁻¹) and 298 K (k_{2app} = 2.6 M s⁻¹).

order kinetics at 273 and 293 K.[28] However, for catalysts **6b** and **6d**, the transition from zero- to second-order kinetics occurs over a wider temperature range. In the case of catalyst **6b**, the kinetics show a decreasingly good fit to zero order and an increasingly good fit to second order as the temperature increases, though only at 293 K is a good fit to second-order kinetics observed and this is better than the fit to zero order at this temperature. A similar trend was seen for the data for catalyst **6d**, though in this case the data at 263 and 273 K fitted only zero-order kinetics, whereas the data at 283 and 293 K could be fitted to either zero- or second-order kinetics with the second-order plot being the slightly better fit at both of these temperatures. However, at 283 and 293 K, the fit of the data to either rate equation was less good than observed in other cases, which suggests that the reaction is transitioning from zero to second order throughout this range and hence does not fit either order particularly well.[28]

Catalyst **1** exhibited first-order kinetics at all temperatures studied (rate = k_{1app}[Me₃SiCN] in which $k_{1app} = k_1$[**1**]$^{1.34}$, as previously determined[27a]). The change in reaction order with temperature prevented any calculation of the enthalpy of activation associated with catalysts **6b–d**, as insufficient points with the same reaction order were available to carry out a reliable graphical analysis.

The Eyring equation [Equation (1)] relates the rate constant (k) for a reaction to the enthalpy ($\Delta H^{\ddagger}$) and entropy ($\Delta S^{\ddagger}$) of activation. However, it is convenient to utilize the apparent rate constants ($k_{app} = k$[catalyst]^x), which are directly available from the variable-temperature kinetics study, so Equation (1) must be modified to give Equation (2). Taking the logarithm of both sides of Equation (2) gives Equation (3), from which it is apparent that $\Delta H^{\ddagger}$ can be determined from the gradient of a plot of ln(k_{app}/T) against $1/RT$ (Figure 3) and that $\Delta S^{\ddagger}$ can be obtained from the y-axis intercept, since the order with respect to the catalyst was determined in the previous section.[38] The thermodynamic data obtained in this way for complexes **1,5** and **6e** are summarized in Table 4.
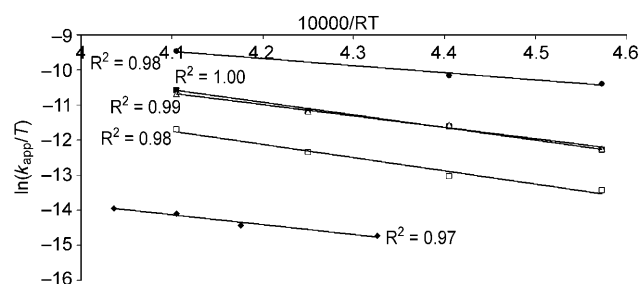
Figure 3. Plots of ln(k_{app}/T) against $1/RT$ for complexes **1,5**, and **6e–g**. **1**: ■, **5**: ◆, **6e**: △, **6f**: □, **6g**: ●.

Table 4. Thermodynamic parameters for complexes **1,5**, and **6e-g**.

Catalyst	$\Delta H^{\ddagger}$ [kJ mol⁻¹]	$\Delta S^{\ddagger}$ [J K⁻¹ mol⁻¹]	$\Delta G^{\ddagger}$ [kJ mol⁻¹][a]
1	35.9	−86	59.4
5	27.6	−184	77.8
6e	32.5	−125	66.6
6f	37.6	−26	44.7
6g	20.4	−136	57.5

[a] At 273 K.

$$k = (k_B \cdot T h^{-1}) \cdot \exp(-\Delta H^{\ddagger}/RT) \cdot \exp(\Delta S^{\ddagger}/R) \qquad (1)$$
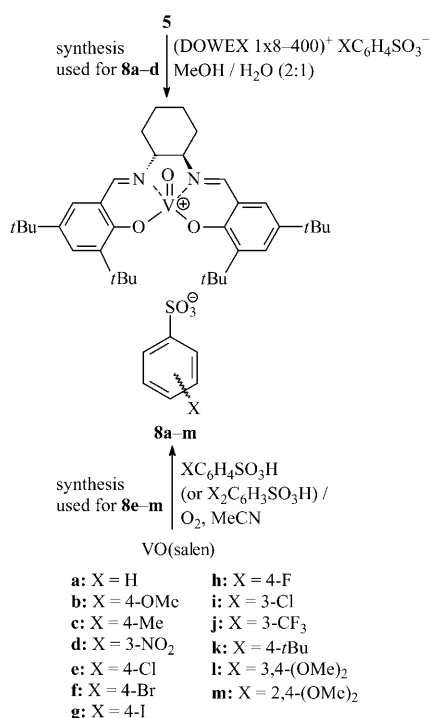
$$k_{app}/T = (k_B h^{-1}) \cdot [\text{catalyst}]^x \cdot \exp(-\Delta H^{\ddagger}/RT) \\ \cdot \exp(\Delta S^{\ddagger}/R) \qquad (2)$$

$$\ln(k_{app}/T) = (-\Delta H^{\ddagger}/RT) + (\Delta S^{\ddagger}/R) \\ + \ln(k_B h^{-1}) + x \ln[\text{catalyst}] \qquad (3)$$

(k_B = Boltzmann's constant, h = Planck's constant, R = gas constant)

The entropies of activation for the vanadium-based catalysts were found to be more negative than that of the titanium-based catalyst **1**. This is consistent with dinuclear species being involved in the catalytic cycles of all of the complexes, as complex **1** is pre-assembled into a dinuclear structure, whereas the vanadium complexes exist predominantly as mononuclear species.

A Hammett correlation study: In view of the unexpected influence of the counterion in complexes **5** and **6a–e** on the catalytic activity of the complexes, a Hammett correlation study was undertaken to confirm the trend within a series of more closely related complexes, and to allow the structure-activity relationship to be quantified.[39] Preliminary studies showed that complexes with benzoate counterions were unstable towards chromatographic purification, so a series of complexes **8a–m** with benzenesulfonate counterions was prepared. Complexes **8a–d** were prepared from complex **5** by ion exchange chromatography on a DOWEX 1X8-400 resin, as discussed above for complexes **6a–c** (Scheme 4). However, attempted preparation of complex **8e** by this method led instead to complex **8b** as a result of a nucleophilic aromatic substitution reaction occurring between 4-chlorobenzenesulfonic acid and the methanol solvent in the

Scheme 4. Synthesis of complexes **8a–m**.

a: X = H
b: X = 4-OMe
c: X = 4-Me
d: X = 3-NO₂
e: X = 4-Cl
f: X = 4-Br
g: X = 4-I
h: X = 4-F
i: X = 3-Cl
j: X = 3-CF₃
k: X = 4-tBu
l: X = 3,4-(OMe)₂
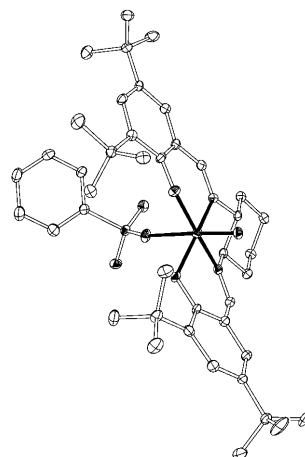**m:** X = 2,4-(OMe)₂

Figure 4. One of the two crystallographically independent molecules of complex **8a**. In all crystallographic figures of molecular structures, hydrogen atoms are omitted for clarity, and displacement ellipsoids are drawn at the 30 % probability level. Bonds to vanadium are shown filled, others hollow.
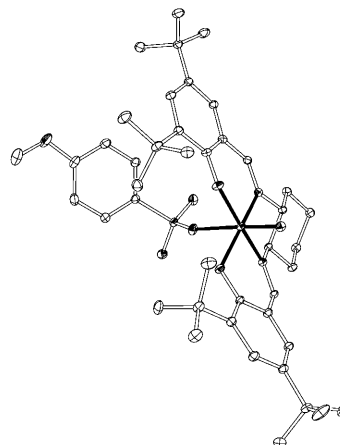

Figure 5. One of the two crystallographically independent molecules of complex **8b**. The close resemblance to the structure of **8a**, in the detailed conformation, is striking.

presence of the basic ion exchange resin. To avoid this problem, an alternative route was used for the preparation of complex **8e**. Thus, treatment of VO(salen)[21b] with two equivalents of 4-chlorobenzenesulfonic acid in acetonitrile, whilst bubbling air through the solution, resulted in oxidation of the vanadium(IV) to vanadium(V) and formation of the desired complex **8e**.[40] This method required less benzenesulfonate than the ion exchange chromatography route, so it was also used for the preparation of complexes **8 f–m** (Scheme 4).

The formation of complexes **8a–m** was confirmed by using ¹H NMR spectroscopy and negative ion mode electrospray mass spectrometry, which indicated the presence of the desired anion. The positive ion mode electrospray mass spectra[28] of complexes **8a–m** again indicated the presence of both mononuclear [VO(salen)]⁺ and dinuclear [VO-(salen)]₂⁺ species as discussed above for complexes **5** and **6a–e**. In addition, complexes **8a** and **8b** formed crystals suitable for analysis by X-ray crystallography (Figure 4 and Figure 5 respectively). The most notable feature of both of these crystal structures is that the benzenesulfonate counterion is directly coordinated to the vanadium ion. The two structures are almost identical, being crystallographically isomorphous. Each has two molecules of the complex and two molecules of toluene in the asymmetric unit. An approximate non-crystallographic inversion center relates the independent molecules, the chirality of the ligand backbone alone breaking this pseudo-inversion symmetry. The absolute configuration is firmly established from the X-ray data on the basis of significant anomalous scattering effects.

Each of complexes **8a–m** was used to catalyze the asymmetric addition of trimethylsilyl cyanide to benzaldehyde under standard conditions (Scheme 3). The resulting rate constants and enantioselectivities are given in Table 5. The enantioselectivity of the addition of trimethylsilyl cyanide to benzaldehyde was again found to be essentially independent of the counterion, with all of complexes **8a–m** giving O-acetyl mandelonitrile with $93 \pm 3 \%$ ee, exactly as observed for complexes **5** and **6b–g** (Table 1). Complexes **8e** and **8f** were found to display zero-order kinetics at 273 K as previously seen for complexes **6b,d** (Table 3). The other complexes all showed good fits to second-order kinetics[28] and the data for complexes **8a–d,g–l** could be used to construct a Hammett plot (Figure 6). The Hammett plot was constructed using apparent second-order rate constants ($k_{2app} = k_2[\text{catalyst}]^x$) and the data gave a good fit ($R^2 = 0.95$) with a

Table 5. Kinetic and enantioselectivity data obtained for complexes **8a–m**.[a]

Complex	Reaction order	Apparent rate constant $\times 10^4$	Enantiomeric excess[b]
8a	2	$k_{2app} = 2.95 \, \text{M}^{-1}\,\text{s}^{-1}$	94 (S)
8b	2	$k_{2app} = 4.72 \, \text{M}^{-1}\,\text{s}^{-1}$	93 (S)
8c	2	$k_{2app} = 3.70 \, \text{M}^{-1}\,\text{s}^{-1}$	94 (S)
8d	2	$k_{2app} = 0.45 \, \text{M}^{-1}\,\text{s}^{-1}$	91 (S)
8e	0	$k_{0app} = 0.65 \, \text{M}\,\text{s}^{-1}$	91 (S)
8f	0	$k_{0app} = 0.62 \, \text{M}\,\text{s}^{-1}$	95 (S)
8g	2	$k_{2app} = 1.97 \, \text{M}^{-1}\,\text{s}^{-1}$	96 (S)
8h	2	$k_{2app} = 2.47 \, \text{M}^{-1}\,\text{s}^{-1}$	94 (S)
8i	2	$k_{2app} = 1.53 \, \text{M}^{-1}\,\text{s}^{-1}$	93 (S)
8j	2	$k_{2app} = 0.93 \, \text{M}^{-1}\,\text{s}^{-1}$	94 (S)
8k	2	$k_{2app} = 4.33 \, \text{M}^{-1}\,\text{s}^{-1}$	96 (S)
8l	2	$k_{2app} = 3.68 \, \text{M}^{-1}\,\text{s}^{-1}$	94 (S)
8m	2	$k_{2app} = 10.50 \, \text{M}^{-1}\,\text{s}^{-1}$	95 (S)

[a] Reactions carried out at 273 ± 0.5 K under the conditions shown in Scheme 3. Apparent rate constants were calculated from the slopes of the appropriate kinetics plots. [b] Determined by chiral GC analysis of mandelonitrile acetate.
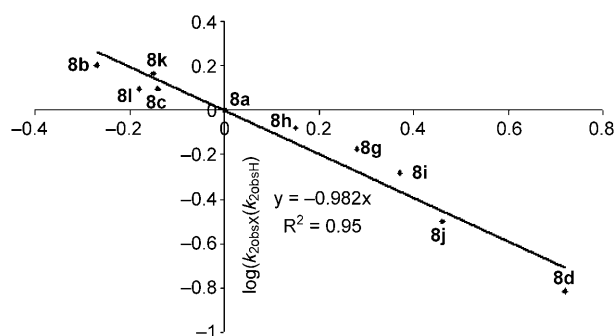
Figure 6. Hammett plot for complexes **8a–d,g–l**.

ρ value of -0.98. As indicated by the negative reaction constant and the rate data in Table 5, complexes **8** with electron-donating substituents formed faster catalysts than the corresponding complexes with electron-withdrawing substituents. The magnitude and sign of the reaction constant are indicative of an increase in positive charge on the sulfur atom during the rate-determining step of the catalytic cycle and this is consistent with electron donation from one of the sulfonate oxygen atoms during this transition state.

The data used to construct the Hammett plot were based on apparent second-order rate constants, as it was not feasible to determine the order with respect to the catalyst for each of complexes **8a–m**. If the order with respect to the catalyst is the same for all of the complexes, then this will cancel out of the equation used to generate the Hammett plot, but if the order varies from catalyst to catalyst then it will result in an apparently non-linear Hammett plot. The good fit to a straight line observed in Figure 6 can be taken as an indication that the order with respect to the catalyst is approximately the same for all of the complexes in this sequence. However, to confirm that this is indeed the case, the order with respect to the catalyst was determined for complexes **8b** and **8i** which bear electron-donating and electron-

withdrawing substituents respectively.[28] This resulted in values of 0.58 and 0.70 respectively, which are sufficiently similar that any error caused by constructing the Hammett plot from observed rate constants rather than actual rate constants would be within the overall experimental error of the experiments and would not affect the conclusions.

Complex **8m** could not be included in the Hammett plot, but it was included in this study, as a test of the predictive powers of the Hammett correlation. Having two methoxy groups present in positions in which they could stabilize positive charge on the sulfur atom through resonance effects was expected to significantly enhance the catalytic activity of the complex. This was indeed found to be the case as the apparent second-order rate constant for complex **8m** was about twice that of complex **8b**, which only has one methoxy substituent. The contrast with complex **8l** was also quite marked as in the latter case one of the methoxy groups is meta to the sulfonate group and hence exerts an electron-withdrawing rather than electron-donating effect. As expected, this reduces the catalytic activity of complex **8l** compared to that of complex **8b**.

Influence of the reaction atmosphere on reactivity: Preliminary studies carried out whilst optimizing the conditions for the kinetics experiments showed that the atmosphere above the reaction was critical to the activity of the catalysts. In particular, attempts to carry out reactions under an argon atmosphere resulted in catalyst deactivation.[20] Thus, for each of complexes **5** and **6c–e**, reactions carried out at 293 K under an argon atmosphere initially exhibited second-order kinetics with an apparent rate constant comparable to that observed for reactions carried out under an air atmosphere. However, after 5–25 minutes reaction, a deviation from second-order kinetics was observed and catalyst deactivation occurred. Catalyst **6d** was found to be totally inactive when used under an argon atmosphere.[28] These data are summarized in Table 6, and a representative set of kinetics results (those for complex **6e**) are shown in Figure 7.

The detrimental effect of an argon atmosphere was however, in some cases, dependent on the reaction temperature. Thus, whilst for catalyst **6c**, reducing the reaction temperature to 273 K still resulted in deactivation, reactions carried out with complex **6e** at 273 K showed no evidence of catalyst deactivation and the reactions obeyed second-order kinetics with an observed rate constant essentially identical to that obtained for reactions carried out under an air atmosphere at the same temperature.

The most likely explanation for these results was that under the reaction conditions, the catalyst was being reduced to catalytically inactive[21b] vanadium(IV) species and atmospheric oxygen was necessary to reoxidize the vanadium(IV) to catalytically active vanadium(V). The lack of deactivation observed for reactions carried out using complex **6e** at 273 K could be a result of the high catalytic activity of this catalyst resulting in catalyst reduction not being significant during the reaction time, though catalyst reduction must be accelerated relative to the rate of catalysis at 293 K

Table 6. Influence of reaction atmosphere on the catalytic activity of complexes **5**, and **6c–g**.

| Complex | Temp. | Reaction order (apparent rate constant $\times 10^4$) | | |
		Argon	Air	Oxygen
5	293 K	$1.8\,M^{-1}s^{-1}$ for first 13% reaction (23 min), then deactivates.	$2.2\,M^{-1}s^{-1}$	
6c	293 K	$13\,M^{-1}s^{-1}$ for first 35% reaction (11 min), then deactivates.	$13\,M^{-1}s^{-1}$	
6c	273 K	$8.5\,M^{-1}s^{-1}$ for first 24% reaction (10 min), then deactivates.	$9.4\,M^{-1}s^{-1}$	$119\,M^{-1}s^{-1}$
6c	263 K		$0.7\,M\,s^{-1}$	$7.8\,M\,s^{-1[a]}$
6d	293 K	no reaction	$1.5\,M^{-1}s^{-1}$	
6e	293 K	$59\,M^{-1}s^{-1}$ for first 52% reaction (5 min), then deactivates.	$67\,M^{-1}s^{-1}$	$98\,M^{-1}s^{-1}$
6e	273 K	$25\,M^{-1}s^{-1}$	$26\,M^{-1}s^{-1}$	$31\,M^{-1}s^{-1}$
6f	273 K	$22\,M^{-1}s^{-1}$ for first 19% reaction (3 min), then deactivates.	$26\,M^{-1}s^{-1}$	
6g	293 K	$157\,M^{-1}s^{-1}$ for first 82% reaction (6 min), then deactivates.	$228\,M^{-1}s^{-1}$	$259\,M^{-1}s^{-1}$
6g	273 K	$103\,M^{-1}s^{-1}$	$105\,M^{-1}s^{-1}$	$111\,M^{-1}s^{-1}$

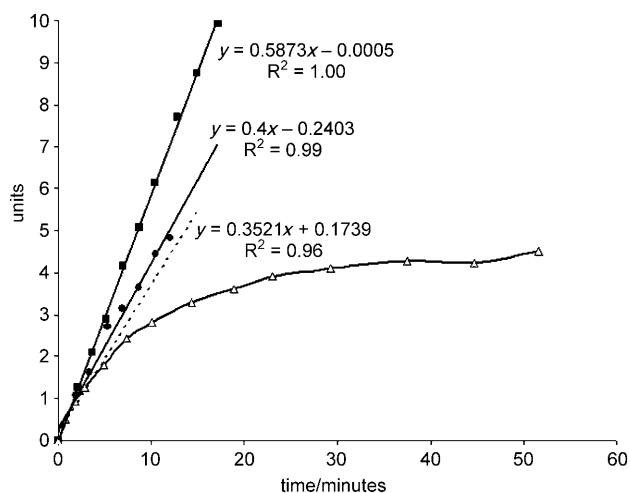[a] Based on first 63% reaction (7 min).

Figure 7. Influence of reaction atmosphere on reactions catalyzed by complex **6e** at 293 K. The hashed line represents the best fit to the linear portion of the reaction carried out under an argon atmosphere. ■: oxygen atmosphere, ●: air atmosphere, △: argon atmosphere. The units used for the vertical scale are: $([PhCHO]_0-[Me_3SiCN]_0)^{-1} \ln([Me_3SiCN]_0[PhCHO]_t[Me_3SiCN]_t^{-1}[PhCHO]_0^{-1})$ where the subscripts 0 and t refer to initial concentrations and concentrations at time t respectively.

to account for the catalyst deactivation observed at the higher temperature.

To investigate the effect of oxygen on the catalytic activity of the complexes in more detail, reactions catalyzed by complexes **6c** and **6e** were carried out under an oxygen atmosphere (Table 6). In the case of catalyst **6c**, this resulted in a greater than tenfold increase in the rate constant at both 273 K (in which reactions under air and oxygen both obeyed second-order kinetics), and at 263 K (in which reactions under air and oxygen both obeyed zero-order kinetics). In contrast, reactions carried out with complex **6e** at 293 K and 273 K showed a much smaller increase in the second-order rate constant on changing the atmosphere from air to oxygen, consistent with catalyst reduction being less significant in this case. However, even in this case, the increase in second-order rate constant was larger at 293 K where catalyst deactivation was observed for reactions carried out under an argon atmosphere than at 273 K at which no catalyst deactivation occurred for reactions carried out under argon.

Stopped flow kinetics: As part of this project we attempted to automate the acquisition of kinetic data by using a stopped-flow kinetics system. Initial reactions showed that it was not possible to monitor the reactions by UV absorbance as, at the concentrations needed for reaction to occur, catalysts **5** and **6a–e** absorbed so strongly that they obscured any change in absorbance, owing to the change in aldehyde concentration. Therefore, the reactions were monitored by fluorescence. Hammock has previously shown that enzymatic hydrolyses of esters of the cyanohydrin of 6-methoxynaphth-2-aldehyde could be followed by fluorescence, as 6-methoxynaphth-2-aldehyde **9** fluoresces strongly at $\lambda = 460$ nm, whereas the corresponding cyanohydrin derivatives fluoresce only weakly below $\lambda = 370$ nm.[41,42] Therefore, the asymmetric addition of trimethylsilyl cyanide to 6-methoxynaphth-2-aldehyde **9** catalyzed by complex **6e** (Scheme 5)
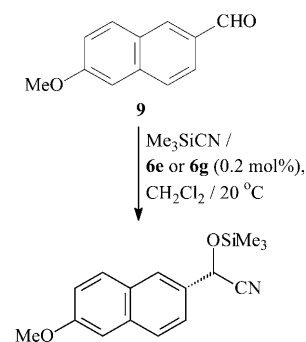
Scheme 5. Asymmetric addition of trimethylsilyl cyanide to aldehyde **9**.

was studied in the stopped flow system, with an absorbance wavelength of $\lambda = 330$ nm and a $\lambda = 395$ nm filter between the cell and detector so that only light with a wavelength $\lambda > 395$ nm and thus arising from fluorescence of aldehyde **9** would be detected. Control experiments confirmed that 6-methoxynaphth-2-aldehyde was a substrate for catalyst **6e** and that it displayed the same kinetic behavior as benzaldehyde (second-order kinetics for reactions carried out in the presence of air, deactivation for reactions carried out under nitrogen).[28]

Based on the above results, it was expected that the fluorescence response would decay as the reaction progressed, corresponding to consumption of the fluorescent aldehyde and that the resulting decay curve would fit a second-order kinetic profile. Since the stopped flow cell is a sealed system, working under anaerobic conditions, it was also anticipated that catalyst deactivation would occur. To avoid saturating the detector, it was necessary to reduce the concentration of the aldehyde, trimethylsilyl cyanide and catalyst by a factor of three for reactions carried out in the stopped flow system, and this was expected to reduce the reaction rate by a factor of 24 for catalyst **6e**. In the event, a large apparent increase in fluorescence was observed, followed by a subsequent decrease in fluorescence intensity which could not be fitted to any simple kinetic profile (Figure 8).
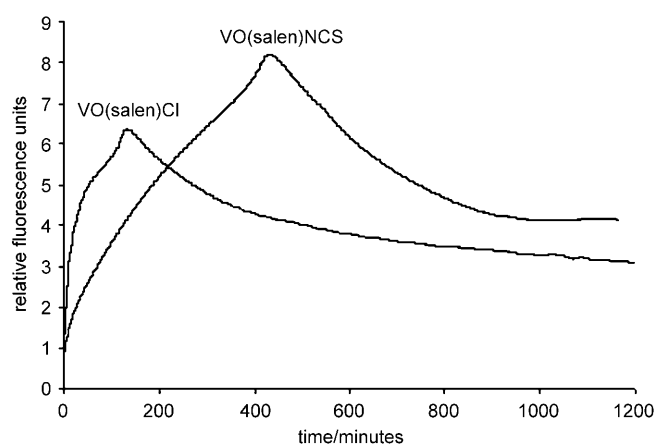

Figure 8. Stopped flow kinetics results obtained using aldehyde **9** and catalyst **6e** or **6g** at 293 K.

The large increase in apparent fluorescence observed during the first 150 minutes of the reaction cannot be a result of an actual increase in fluorescence, as the concentration of aldehyde **9** is at a maximum at the start of the reaction. However, the UV spectra[28] of VO(salen) and complex **6e** showed that the extinction coefficient of complex **6e** is greater than that of VO(salen) at all wavelengths above $\lambda = 325$ nm, so the observed increase in fluorescence is consistent with a decrease in the absorbance of the incident radiation ($\lambda = 330$ nm; VO(salen) $\varepsilon_{330} = 3813$, **6e** $\varepsilon_{330} = 10558$) and/or the radiation arising from fluorescence ($\lambda = 460$ nm; VO-(salen) $\varepsilon_{460} = 257$, **6e** $\varepsilon_{460} = 2019$) as a result of the in situ reduction of vanadium(V) to vanadium(IV). Thus the stopped-flow kinetics study provided additional evidence to support the in situ formation of vanadium(IV) containing species during the catalytic cycle. The remainder of the data in Figure 8 are consistent with a second-order reaction between aldehyde **9** and trimethylsilyl cyanide accompanied by catalyst deactivation (Table 6).

Cyclic voltammetry: As the experiments carried out under different atmospheres and the stopped flow kinetics results both suggested that the oxovanadium(V)(salen) complexes may be reduced to the corresponding oxovanadium(IV)-(salen) complexes in situ, this process was investigated by cyclic voltammetry to see if there was a correlation between the catalytic activity of the complexes and their reduction potential. The electrochemical properties of oxovanadium-(salen) complexes have been extensively studied[24, 25, 30, 37c–e, 40, 43] and it is well established that the interconversion between vanadium(IV) and vanadium(V) species is electrochemically reversible and occurs in dichloromethane solution in the presence of a tetraalkylammonium electrolyte.

Complexes **6b–e** were selected for electrochemical study. This series included all of the complexes which displayed zero-order kinetics (Table 3), as well as the highly active complex **6e**. The cyclic voltamogram of each complex was recorded at 22°C as a 0.6–1.1 mM solution in dichloromethane in the presence of a 0.1 M solution of the corresponding tetrabutylammonium salt and under a nitrogen atmosphere.[28] The use of dichloromethane as solvent meant that the observed redox behavior was likely to be relevant to catalytic reactions carried out in dichloromethane. Table 7

Table 7. Redox potentials of complexes **6b–e,g** determined by cyclic voltammetry.[a]

Complex	Redox potential [mV]
6b	−111
6c	−229
6d	−197
6e	−239
6g	−515[b]

[a] Relative to ferrocene. Scan rate 100 mV s^{-1}. [b] Approximate value as redox wave is weak.

gives the redox potentials of complexes **6b–e** relative to that of ferrocene. It is apparent from Table 7 that the three catalysts which exhibit zero-order kinetics at temperatures below 293 K (**6b–d**) all have less negative reduction potentials than complex **6e** and hence are more prone to reduction to catalytically inactive vanadium(IV) species during a catalytic reaction. This is consistent with reoxidation of vanadium(IV) to catalytically active vanadium(V) being the rate-determining step in the catalytic cycle at lower temperatures for complexes **6b–d**, whilst for complex **6e** this reoxidation is less significant.
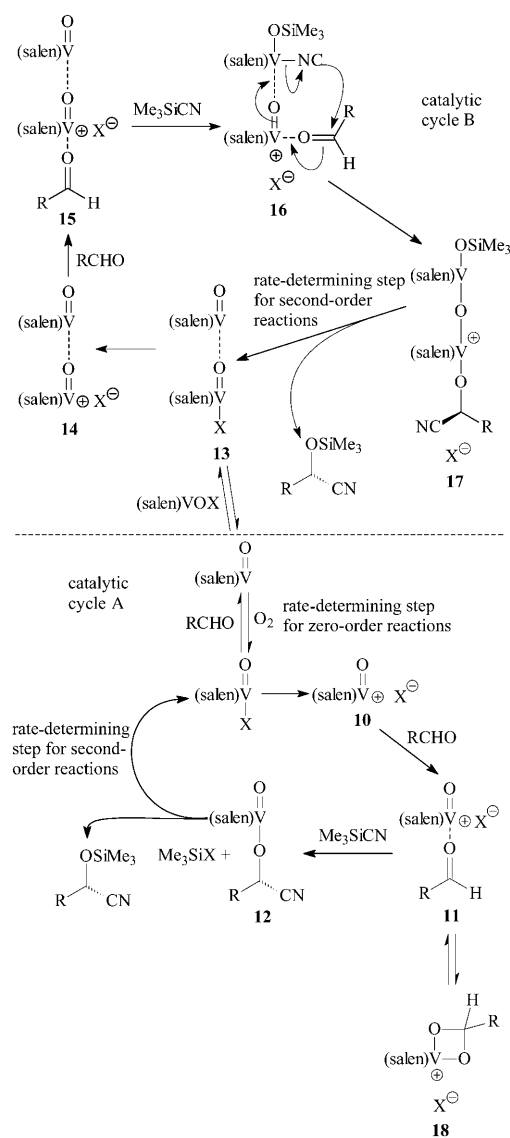
Catalytic cycles: Any catalytic cycle to explain the mode of action of complexes **5**, **6**, and **8** must be compatible with the following features of the chemistry.

- The structure of the counterion X$^-$ in complexes of general structure VO(salen)$^+$ X$^-$ significantly affects the rate of reaction but not the asymmetric induction.

- The more nucleophilic the counterion, the faster the rate of the catalyzed reaction.
- Both mononuclear and binuclear species are present in solution and both may be catalytically active.
- Reactions catalyzed by some VO(salen)$^+$ X$^-$ complexes exhibit second-order kinetics whilst others exhibit zero-order kinetics.
- The catalysts undergo reduction in situ to vanadium(IV)-(salen) complexes.
- Mononuclear vanadium(IV)(salen) complexes (VO-(salen)) are known to be catalytically inactive for asymmetric cyanohydrin synthesis under the conditions used for complexes **5**, **6**, and **8**.[21b]

As the order with respect to the catalyst data (Table 2) suggests that catalysts **5**, **6**, and **8** are at least partly catalytically active as mononuclear species, the catalytic cycle shown in Scheme 6 (catalytic cycle A) can be used to explain some of the experimental features.[44] In this catalytic cycle, complexes **5**, **6**, and **8** first dissociate the counterion or coordinated water molecule to form complex **10** which was detected by mass spectrometry.[28] Complex **10** is coordinatively unsaturated and can act as Lewis acid, coordinating to the aldehyde to form species **11**. The activated aldehyde within complex **11** can then undergo intermolecular attack by cyanide to form the new stereocenter and give a vanadium bound cyanohydrin derivative **12**. Expulsion of the cyanohydrin from complex **12** by the counterion and silylation would generate the cyanohydrin trimethylsilyl ether and regenerate complexes **5**, **6**, and **8**. If the rate-determining step of this catalytic cycle is the recoordination of the counterion to complex **12** with extrusion of the cyanohydrin, then overall second-order kinetics (rate = k[RCHO][Me$_3$SiCN]) would be observed and the rate of reaction would be determined by the coordinating ability of the counterion. This catalytic cycle also explains why the asymmetric induction is independent of the nature of the counterion, since the counterion is a spectator in the conversion of complex **11** into complex **12** during which the stereocenter is created. The fact that complexes **5**, **6**, and **8** form much less active catalysts than titanium-based complex **1** is also consistent with this catalytic cycle, as the previously determined[27] mechanism for complex **1** involves activation of both the aldehyde and cyanide and intramolecular transfer of cyanide to the aldehyde. In contrast, the vanadium-based catalysts are only activating the aldehyde in catalytic cycle A of Scheme 6.

The need for an oxygen atmosphere can also be accommodated by catalytic cycle A of Scheme 6. Thus, complexes **5**, **6**, and **8** can also oxidize an aldehyde[45] and in the process are reduced to the catalytically inactive vanadium(IV) complex VO(salen). Molecular oxygen then reoxidizes this complex to the catalytically active vanadium(V) species. For those complexes that have low reduction potentials (**6b–d**, see Table 7), this reoxidation can become the rate-determining step and, hence, the reactions exhibit over all zero-order kinetics. Further support for this hypothesis came from a reaction in which acetophenone was employed as substrate.

Scheme 6. Catalytic cycles for asymmetric cyanohydrin synthesis using complexes **5**, **6**, and **8**.

Catalyst **1** is known to accept methyl ketones as substrates, though the reactions require a higher catalyst loading (0.5 mol%) and longer reaction time (24 h) than those used for aldehyde substrates.[6a, 18b] However, use of 0.5 mol% of catalysts **6** with acetophenone gave at most a 20% yield (*ee* not determined) after a reaction time of four days. This suggests that catalytic cycle A cannot fully account for catalysis by the more active of the vanadium-based catalysts such as **6e**.

The order, with respect to catalyst data (Table 2) and the mass spectrometry data, indicate that the mononuclear complexes present in catalytic cycle A are in equilibrium with dinuclear species and the acetophenone results are consistent with the vanadium(V)-based catalysts requiring in situ reduction to a mixed vanadium(IV)–vanadium(V) dimer to form the most active catalysts. A ketone would be unable to act as the reducing agent for this process and, hence, be

unable to activate precatalysts **6**. Subsequent results (vide infra) and literature precedent based on the corresponding dinuclear titanium salen complexes[27] and heterobimetallic titanium–vanadium salen complexes[27b] strongly suggested that dinuclear complexes would form highly-active catalysts.

Scheme 6 can be extended to include a second catalytic cycle (catalytic cycle B) based on dinuclear complexes. Thus, coordination of the in situ formed vanadium(IV) complex VO(salen) with a second molecule of complexes **5**, **6**, and **8** forms dinuclear complex **13** which contains one vanadium(IV) ion and one vanadium(V) ion. Dissociation of the counterion from complex **13** leads to the monocharged dinuclear complex **14**, which was detected by mass spectrometry.[28] Coordination of the aldehyde to the coordinatively unsaturated vanadium(V) ion of complex **14** gives complex **15**. In contrast to catalytic cycle A, it is now possible for the trimethylsilyl cyanide to react with the vanadium(IV) ion of complex **15** leading to complex **16**,[46] which is able to transfer cyanide intramolecularly to the coordinated aldehyde in the same way as previously described[27a] for titanium-based complex **1**. This would form complex **17** containing a vanadium-bound cyanohydrin. Expulsion of the cyanohydrin by the counterion and silylation regenerates complex **13** and forms the cyanohydrin trimethylsilyl ether product. As for the mononuclear cycle (cycle A), if the conversion of complex **17** to **13** is the rate-determining step of the catalytic cycle then overall second-order kinetics will be observed and the relative reactivities of complexes **5** and **6a–e** will be explained. The observation of zero-order kinetics in some cases is also consistent with this catalytic cycle as this would correspond to the reoxidation of VO(salen) to VO(salen)X being the rate-determining step, the latter being required for the formation of dinuclear complex **13**.

The asymmetric induction observed in the bimetallic catalytic cycle is readily understood on the basis of the previously reported transition state for titanium-based complex **1**.[27] Intramolecular cyanide transfer is only possible if both salen ligands adopt the *cis*-β configuration,[47,48] thus allowing the coordinated aldehyde and cyanide to both be located *cis* to the bridging oxygen atom. The higher level of asymmetric induction observed with vanadium complexes may be due to formation of a tighter transition state, owing to the extra positive charge of the vanadium ion to which the benzaldehyde is coordinated. It is however, a feature of catalysts **5**, **6**, and **8** that the level of asymmetric induction is independent of the order with respect to the catalyst (Tables 1, 2 and 5), which suggests that in both catalytic cycles the new stereocenter is created in a similar chiral environment. During the conversion of complex **11** to complex **12**, the salen ligand is apparently able to adopt a planar configuration around the vanadium ion, which would not be expected to result in the same level of asymmetric induction as obtained from catalytic cycle B. However, coordinated aldehyde **11** can be in equilibrium with a metalloacetal-containing species **18**.[49] This would force the salen ligand into the *cis*-β configuration[50] and account for the observed asymmetric induction. Although it has not proven possible to detect complex **18**,

the corresponding titanium-based complex has previously been detected.[27a]

Thus, the two catalytic cycles shown in Scheme 6 allow all of the features of asymmetric cyanohydrin synthesis catalyzed by VO(salen)X complexes to be explained. They could be tested and also allowed predictions to be made as to how the catalytic activity of VO(salen)X complexes could be enhanced to a level comparable with that of complex **1** as discussed below.

Influence of added tetrabutylammonium chloride: The rate-determining step for both catalytic cycles in Scheme 6 involves the counterion acting as a nucleophile and displacing the cyanohydrin trimethylsilyl ether from complexes **12** and **17** respectively. Therefore, if these catalytic cycles are correct, carrying out the reaction in the presence of an excess of the counterion should result in a rate enhancement. To test this, reactions were carried out with catalyst **6e** in the presence of varying concentrations of tetrabutylammonium chloride. As ammonium halides are known to catalyze the racemic addition of trimethylsilyl cyanide to aldehydes,[51] a control experiment was first carried out in which tetrabutylammonium chloride was the only catalyst employed. This showed that under the reaction conditions used (Scheme 3), the reaction catalyzed by tetrabutylammonium chloride (1 mol %) was 40 times slower than that catalyzed by complex **6e** (0.2 mol %). If tetrabutylammonium chloride (0.01–2 mol %) was added to reactions catalyzed by complex **6e** (0.2 mol %) it did however have a remarkable effect on the rate of reaction, as shown in Figure 9.[28] In the presence of 0.1 mol % or more of tetrabutylammonium chloride, the reaction kinetics changed from second to first order and a rate enhancement was observed as expected.[52] However, if more than 0.4 mol % of tetrabutylammonium chloride was used then the reaction rate started to decrease, though even when 2 mol % of tetrabutylammonium chloride was used the rate was more than 50 % faster than if no tetrabutylammonium chloride was employed. The enantioselectivity of these reactions did not vary and was consistently 96–97 %.
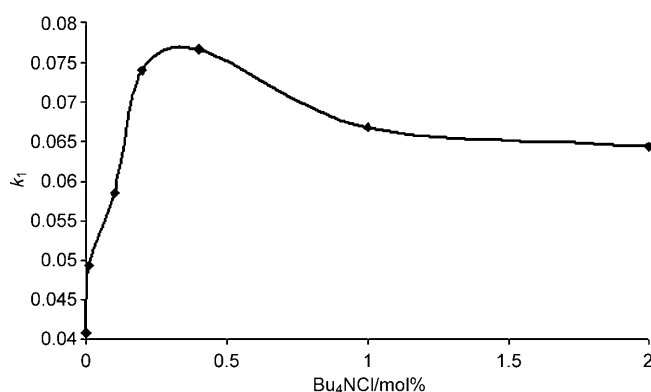

Figure 9. Influence of added tetrabutylammonium chloride on the first-order rate constant for the asymmetric addition of trimethylsilyl cyanide to benzaldehyde catalyzed by complex **6e** at 273 K.

The results shown in Figure 9 are entirely consistent with the catalytic cycles shown in Scheme 6. Therefore, although increasing the concentration of chloride will increase the rate of the rate-determining step for both catalytic cycles, eventually the rate of this step will be enhanced to such an extent that it is no longer the rate-determining step of the catalytic cycle. Adding excess chloride will also have a second effect on the catalytic cycle: it will slow down the rate at which benzaldehyde coordinates to the catalyst (formation of **11** and **15**), because the chloride will compete with benzaldehyde to coordinate to complexes **10** and **14**. The effect of this will be to increase the rate at which species **11** and **15** are converted back to VO(salen)X and complex **14** respectively, and thus to reduce the concentrations of species **11** and **15**. This second effect explains why, at higher concentrations of chloride, the rate of reaction decreases and also why the kinetics change from second to first order, since if coordination of benzaldehyde to the catalyst is the rate-determining step of the catalytic cycle then the rate will be independent of the concentration of trimethylsilyl cyanide.

Mechanism-based development of new highly active catalysts: Based on the kinetic results obtained with complexes **5**, **6a–e**, and **8a–m**, and the catalytic cycles postulated in Scheme 6, it is possible to predict the properties needed in a counterion X to make the corresponding VO(salen)X complex a highly active catalyst for asymmetric cyanohydrin synthesis. A good counterion should encourage the formation of bimetallic (or oligomeric) complexes and should have a strong propensity to bind to the vanadium(V) ion so as to increase the rate of the rate-determining step of the catalytic cycle. In particular, it is apparent from the data in Table 2 that complexes **5** and **6b–e** are catalytically active predominantly or exclusively as mononuclear species. In contrast, complex **1**, which has a much higher rate of catalysis than any of the vanadium-based catalysts, is known to be catalytically active as a dinuclear species.[27a] Therefore, if the main cycle of catalysis could be switched from cycle A of Scheme 6 to cycle B, then a significant increase in reaction rate could be anticipated.

A search of the Cambridge Structural Database[53] revealed two promising counterions. Thus, the crystal structures of known VO(salen)F complexes all had polynuclear structures with tetrafluoroborate or VO_2F_2 anions also present. However, in each case the fluoride ion acted as a bridging ligand between two vanadium ions to which it was directly coordinated.[29,54] An achiral VO(salen)NCS complex has also been prepared and its crystal structure showed that the isothiocyanate ligand was directly bound to the vanadium ion.[55] Therefore, the synthesis of complexes **6f** and **6g** was undertaken in the expectation that they would both form highly active catalysts for asymmetric cyanohydrin synthesis.

Complex **6f** was prepared by treatment of salen ligand **7** with vanadium oxyfluoride (Scheme 2). The nature of the solvent was critical for the success of this procedure. Use of

THF as the reaction solvent, as used for the synthesis of complex **6e**, gave a highly impure product when used for the synthesis of complex **6f**. However, treatment of ligand **7** with vanadium oxyfluoride in dichloromethane gave complex **6f** in high purity with no need for chromatographic purification, which was critical to the success of the synthesis, as complex **6f** was found to be unstable to silica gel chromatography. Complex **6g** was conveniently prepared simply by treatment of complex **5** with an ethanolic solution of potassium thiocyanate. In this case the success of the ion exchange procedure was confirmed by X-ray crystallography (Figure 10), which clearly showed the presence of the isothiocyanate unit directly bound to the vanadium ion through the nitrogen atom as previously reported for a similar VO(salen)NCS complex.[55] The crystal structure of **6g** contains four independent complex molecules and four molecules of toluene in the asymmetric unit. The absolute configuration is unambiguously established from anomalous scattering effects.

Figure 10. The structure of one of the four crystallographically independent molecules of complex **6g**.

As the data in Figure 1 and Table 1 confirm, both complexes **6f** and **6g** were indeed highly-active catalysts for the asymmetric addition of trimethylsilyl cyanide to benzaldehyde. Complex **6f** was not as active as chloride complex **6e**, but was much more active than any of the other catalysts prepared in this project. In contrast, complex **6g** was found to be by far the most active vanadium-based catalyst yet developed for asymmetric cyanohydrin synthesis with an apparent second-order rate constant more than three times greater than that of complex **6e** (the second most active catalyst). Both complexes **6f** and **6g** also retained the high level of asymmetric induction observed for other oxovanadium(V)(salen) complexes (Table 1). Experiments carried out with catalyst **6g** and varying concentrations of benzaldehyde and trimethylsilyl cyanide confirmed that reactions with this catalyst still obeyed the rate equation: rate $= k_{2app}$[PhCHO][Me$_3$SiCN].[28]

The high-resolution electrospray mass spectra of complexes **6f** and **6g** showed the presence of both mononuclear [VO(salen)]$^+$ and dinuclear [(VO(salen))$_2$]$^+$ ions, the latter containing both vanadium(V) and vanadium(IV) ions as previously observed for complexes **6a–e** and **8a–m**.[28] However, the mass spectrum of complex **6f** also showed peaks corresponding to higher oligomers (up to a tetramer detected) and the ^{1}H, ^{13}C and ^{19}F NMR spectra of complex **6f** were all significantly broader than those of the other VO(salen)X catalysts, consistent with the existence of oligomeric species in solution.[29,54]
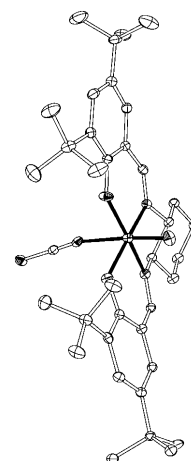
The order with respect to the catalyst was determined for both complexes **6f** and **6g** to further investigate their propensity for formation of oligomeric species (Figure 2 and Table 2).[28] For complex **6f**, the order with respect to the catalyst was found to be 2.4, a value which is much higher than that found for any other vanadium (or titanium) complex and implies that species containing three or more vanadium ions are involved in the catalysis.[56] The highly catalytically active complex **6g** was found to have an order with respect to the catalyst of 1.23 which is significantly higher than the value obtained for any other oxovanadium(salen) complex except **6f** and is comparable to the value observed for complex **1**. This indicates that a dinuclear species is the predominant catalytically active form in the case of this catalyst and the high level of catalytic activity observed with complex **6g** is consistent with the catalytic cycles outlined in Scheme 6 in which bimetallic species are more active than mononuclear species. Again however, mononuclear species are also present in the reaction and these may have some catalytic activity.

A variable-temperature study of the kinetics of the asymmetric addition of trimethylsilyl cyanide to benzaldehyde catalyzed by complexes **6f** and **6g** was also highly informative (Figure 3 and Table 4).[28] Complex **6f** was found to have a much less negative entropy of activation ($-26 \, \mathrm{J\,K^{-1}\,mol^{-1}}$) than any of the other complexes. However, this is entirely consistent with de-oligomerization of the complex during the assembly of the key catalytically active species, which would partly offset the decrease in entropy associated with bringing the catalyst and two reactants together. The high catalytic activity of complex **6g** is largely enthalpic in nature as its enthalpy of activation is exceptionally low, even compared to the highly active titanium-based catalyst **1**. The result of this is that complex **6g** has a low Gibbs energy of activation even though its entropy of activation is higher than that of either complex **1** or complex **6e**.

The thermodynamic data in Table 4 suggest that complex **6f** should be the most active catalyst studied as it has the lowest Gibbs energy of activation. However, both complexes **6e** and **6g** are more active than complex **6f**. This may be due to only a relatively small amount of the oligomeric precatalyst **6f** being converted into a catalytically active species during the catalytic cycle and hence to the concentration of active catalyst present in the reaction being much lower in the case of catalyst **6f** than for any of the other complexes. For complexes **1**, **5**, **6e**, and **6g**, the trend in Gibbs energy of activation (**5** > **6e** > **1** > **6g**) does correspond to the observed relative catalytic activities (**5** < **6e** < **1** < **6g**).

The influence of the reaction atmosphere on catalysis by both complexes **6f** and **6g** was also investigated (Table 6).[28] In the case of catalyst **6f**, changing the atmosphere from air to argon at 273 K deactivated the catalyst exactly as seen for complex **6c**. In the case of the more active catalyst **6g** however, the results resembled those discussed above for complex **6e**. Thus, at 293 K, deactivation occurs when reactions are carried out under an argon atmosphere, whereas

use of an oxygen atmosphere results in a 13% rate enhancement compared to reactions carried out under air. However, at 273 K, no deactivation occurred under an argon atmosphere and no significant rate enhancement was observed when an oxygen atmosphere was used. Thus, at 273 K, complex **6g** is such an active catalyst for asymmetric cyanohydrin synthesis that the reaction is complete before reductive processes can have any influence on the reaction.

The cyclic voltamogram of complex **6g** was consistent with this analysis as the complex was found to have a very negative reduction potential ($-515 \, \mathrm{mV}$) compared to complexes **6b–e**. This indicates that complex **6g** is significantly less prone to reduction to catalytically inactive vanadium(IV) species than any of the other VO(salen)X species studied. Use of complex **6g** under stopped flow conditions (Scheme 5) also indicated that reduction of complex **6g** was more difficult than reduction of the other VO(salen)X complexes. The time dependence of the fluorescence (Figure 8) showed the same increase followed by decrease in intensity as seen for complex **6e**, but the maximum fluorescence intensity for complex **6g** was observed after 430 minutes, whereas that for complex **6e** occurred after just 130 minutes. The UV spectrum of complex **6g** closely resembled that of complex **6e** with $\varepsilon_{330} = 11\,458$ and $\varepsilon_{460} = 2478$.[28]

Asymmetric cyanohydrin synthesis using catalyst 6g: Having developed complex **6g** as the most active vanadium-based catalyst for the asymmetric addition of trimethylsilyl cyanide to benzaldehyde, its application to the asymmetric synthesis of a range of other cyanohydrin trimethylsilyl ethers was investigated. These reactions were carried out using the (*S,S*)-enantiomer of catalyst **6g** under the standard synthetic conditions used previously[6,18] (0.1 mol% catalyst, dichloromethane, room temperature, air atmosphere) to allow comparison with previous results and to demonstrate the effectiveness of the catalyst under convenient reaction conditions and at a high substrate to catalyst ratio. The reactions were stopped after a 2 hour reaction time and the cyanohydrin trimethylsilyl ether was isolated and purified, then converted into the corresponding cyanohydrin acetate[26] to allow its *ee* to be determined (Scheme 7). The results obtained with thirteen different aldehydes **19a–m** are shown in Table 8.

As expected, use of the (*S,S*)-enantiomer of catalyst **6g** always resulted in the preferential addition of cyanide to the
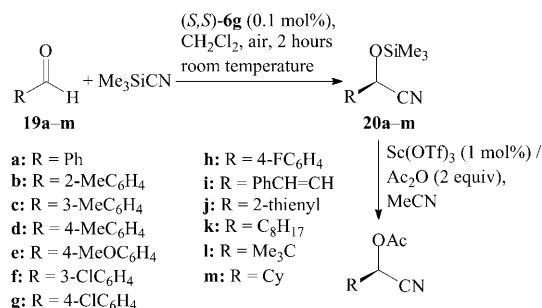
Scheme 7. Asymmetric cyanohydrin synthesis using (*S,S*)-**6g**.

Table 8. Asymmetric cyanohydrin synthesis using aldehydes **19a–m**[a]

Aldehyde	Yield of **20a–m** [%]	ee [%] [b]	Lit ee [%]
19a	99	91 (R)	94,[f] 86[g]
19b	99	88 (R)	90,[f] 76[g]
19c	94	92 (R)	95,[f] 90[g]
19d	99	91 (R)	94,[f] 87[g]
19e	98	>95[c]	90,[f] 84[g]
19f	93	87[d]	
19g	99	86 (R)	
19h	94	92[d]	
19i	93	85 (R)	
19j	96	81[c] (S)[e]	
19k	93	87 (R)	
19l	98	79 (R)	68,[f] 66[g]
19m	85	85 (R)	

[a] All reactions were carried out at room temperature for 2 h using 0.1 mol % of catalyst **6g** in dichloromethane. [b] Determined by chiral GC analysis of the cyanohydrin acetate unless stated otherwise. [c] Based on comparison of the specific rotations of the trimethylsilyl ethers with literature values for **19e**[57] and **19j**.[58] [d] Absolute configuration unknown but assumed to be R based on the order of elution of the major and minor peaks from the chiral GC column. [e] The formation of the (S)-enantiomer in this case is purely an artifact of the CIP priority rules. [f] Value for cyanohydrin trimethylsilyl ethers obtained using catalyst **5**.[18b] [g] Value for cyanohydrin trimethylsilyl ethers obtained using catalyst **1**.[6a]

si-face of the aldehyde. The enantioselectivities obtained with catalyst **6g** were generally comparable to those previously reported[18b] using catalyst **5** and significantly higher than those obtained[6a] using catalyst **1**, but the reactions had mostly gone to completion in two hours, as opposed to the 24 h required using catalyst **5**. The only exception to this trend was pivaldehyde **19l**, which gave a much higher enantioselectivity with catalyst **6g** than that obtained with either catalyst **1** or **5**. One reason for this may be that the much shorter reaction time required when using catalyst **6g** prevents the racemic background reaction from occurring to any significant extent and so raises the observed enantioselectivity.

Conclusion

Oxovanadium(V)(salen) complexes have been shown to catalyze the asymmetric addition of trimethylsilyl cyanide to aldehydes by two parallel catalytic cycles involving monometallic and bimetallic catalytic species respectively. The bimetallic pathway involves cooperative metal ion catalysis by vanadium ions in two different oxidation states and leads to intrinsically faster catalysts, as both components of the reaction (aldehyde and cyanide) are simultaneously activated and assembled for reaction. The key step in both catalytic cycles is the displacement of the metal-bound cyanohydrin from vanadium by the counterion present in the vanadium complex. It has also been shown that atmospheric oxygen plays a key role in the catalysis, by maintaining the required equilibrium between vanadium(IV) and vanadium(V) species.

The determining of the catalytic cycles allowed a catalyst with optimized structure to be designed and resulted in the development of VO(salen)NCS **6g** as the most active vanadium-based catalyst for asymmetric cyanohydrin synthesis yet developed. Complex **6g** was found to catalyze the asymmetric addition of trimethylsilyl cyanide to aromatic and aliphatic aldehydes at a rate which is comparable to that of bimetallic titanium(salen) complex **1** and did so with enantioselectivities comparable to those previously observed for other vanadium-based catalysts.

Experimental Section

General procedure for aldehyde cyanosilylation by the (*S*,*S*)-enantiomer of catalyst 6g: Aldehyde **19a–m** (0.98 mmol) was added to a solution of catalyst (*S*,*S*)-**6g** (0.66 mg, 0.98 μmol, 0.1 mol %) in dry CH_2Cl_2 (1.75 mL) at room temperature. Trimethylsilyl cyanide (0.15 mL, 1.12 mol) was then added. The reaction mixture was stirred for 2 h, then filtered through a plug of silica eluting with CH_2Cl_2 and evaporated in vacuo. If any unreacted aldehyde was present, the residue was purified by rapid chromatography on silica eluting with toluene/ethyl acetate (see the Supporting Information for details) to give cyanohydrin trimethylsilyl ethers **20a–m**. Compounds **20a–m** were subsequently dissolved in MeCN (1 mL) and $Sc(OTf)_3$ (5 mg, 0.01 mmol) and acetic anhydride (0.2 mL, 2.1 mmol) were added. After 20 minutes, the reaction mixture was passed through a short silica plug eluting with MeCN. The resulting solution of the cyanohydrin acetate was analyzed by GC to determine the enantioselectivity of the cyanosilylation.

General procedure for kinetics experiment: A solution of a catalyst (1.96 μmol, 0.2 mol %) in dry dichloromethane (1.75 mL) was added to a round-bottomed flask fitted with a magnetic stirrer bar and a SubaSeal stopper. For reactions in a non-air atmosphere, the flask had been thoroughly flushed with argon or oxygen before the addition of the catalyst solution. The reaction temperature was adjusted by a water bath (water-ice for 0°C; water-ethanol for −10°C; temperatures other than 0°C were kept within a ±0.5°C range by adding dry ice). Bu_4NCl (0.96–19.2 μmol) was added for experiments carried out in the presence of excess chloride. A 0.5 μL aliquot was taken and diluted into dry dichloromethane (3.5 mL). This solution was used for UV-baseline calibration at 240–260 nm. Freshly distilled benzaldehyde (0.1 mL, 0.96 mmol) was then added and a $t=0$ aliquot was taken and analyzed as described for the baseline calibration sample. Trimethylsilyl cyanide (0.15 mL, 1.125 mmol) was added, and aliquots of the reaction were taken at approximate intervals of $t=1, 2.5, 5, 7.5, 10, 12.5, 15, 20, 25$ and 30 minutes and each 10 minutes thereafter if necessary. After completion of the kinetics analysis, the reaction mixture was passed through a short silica plug eluting with dichloromethane. The solvent was evaporated and the residue dissolved in MeCN (1 mL) and $Sc(OTf)_3$ (5 mg, 0.01 mmol) and acetic anhydride (0.2 mL, 2.1 mmol) were added. After 20 minutes, the reaction mixture was passed through a short silica plug eluting with MeCN. The resulting solution was analyzed by GC to determine the enantioselectivity of the cyanosilylation. GC conditions: initial temperature 100°C, hold at initial temperature for 5 minutes, then ramp rate 5°C min⁻¹. $T_R=15.5$ min (R-enantiomer) and 15.7 min (S-enantiomer).

Typical procedure for stopped flow kinetics experiments: The system was thoroughly flushed with CH_2Cl_2 and held at 293 K using a thermostated water bath. The incident light was passed through a monochromator to select a wavelength of 330 nm and a 395 nm filter was inserted between the stopped flow cell and the fluorescence detector. Syringe A was charged with aldehyde **9** (180 mg, 0.97 mmol) in CH_2Cl_2 (3 mL) and syringe B was charged with trimethylsilyl cyanide (0.14 mL, 1.05 mmol) and complex **6e** (1.15 mg, 1.78 μmol) or complex **6g** (1.19 mg, 1.78 μmol) in CH_2Cl_2 (3 mL). The system was then flushed with the contents of syringe B to obtain the background measurements. The experiment was started simultaneously by pneumatically driving samples from both sy-

ringes into the reaction cell and the fluorescence was monitored over a period of 20 h.

X-ray crystallography: Data for compounds **8a**, **8b**, and **6g** were measured at 120 K with synchrotron radiation at the Daresbury Laboratory Synchrotron Radiation Source. Details are provided in the Supporting Information. The structures were solved by standard direct methods and refined on all unique F^2 values. Each structure contains multiple molecules in the crystallographic asymmetric unit ($Z' = 2$, 2, and 4 respectively), and all are 1:1 toluene solvates; one toluene molecule in **8a** could not be modeled with discrete atoms. CCDC 698433 (**8a**), 698434 (**8b**), 698435 (**6g**) contain the supplementary crystallographic data for this paper. These data can be obtained free of charge from The Cambridge Crystallographic Data Centre via www.ccdc.cam.ac.uk/data_request/cif.

[1] L. Rosenthaler, *Biochem. Z.* **1908**, *14*, 238–253.

[2] For reviews see: a) R. J. H. Gregory, *Chem. Rev.* **1999**, *99*, 3649–3682; b) M. Schmidt, H. Griengl, *Top. Curr. Chem.* **1999**, *200*, 193–226; c) F. Effenberger, *Chimia* **1999**, *53*, 3–10; d) F. Effenberger, S. Forster, H. Wajant, *Curr. Opin. Biotechnol.* **2000**, *11*, 532–539; e) H. Griengl, H. Schwab, M. Fechter, *Trends Biotechnol.* **2000**, *18*, 252–256; f) M. H. Fechter, H. Griengl, *Food Technol. Biotechnol.* **2004**, *42*, 287–294; g) K. Gruber, C. Kratky, *J. Polym. Sci. Part A* **2004**, *42*, 479–486; h) J. Sukumaran, U. Hanefeld, *Chem. Soc. Rev.* **2005**, *34*, 530–542; i) M. Sharma, N. N. Sharma, T. C. Bhalla, *Enzyme Microb. Technol.* **2005**, *37*, 279–294.

[3] a) S. C. Stinson, *Chem. Eng. News* **2001**, *79*, (issue 50), 35–38; b) H. Gröger, *Adv. Synth. Catal.* **2001**, *343*, 547–558; c) A. J. Blacker, M. North, *Chem. Ind.* **2005**, 22–25.

[4] a) M. North, *Synlett* **1993**, 807–820; b) M. North, *Tetrahedron: Asymmetry* **2003**, *14*, 147–176; c) J.-M. Brunel, I. P. Holmes, *Angew. Chem.* **2004**, *116*, 2810–2837; *Angew. Chem. Int. Ed.* **2004**, *43*, 2752–2778; d) M. North, D. L. Usanov, C. Young, *Chem. Rev.* **2008**, *108*, 5146–5226.

[5] Throughout this manuscript "salen" refers to the ligand obtained by removing the two phenolic protons from *N*,*N*′-(3,5-di-*tert*-butylsalicylidene)-(*R*,*R*)-1,2-diaminocyclohexane **7**.

[6] a) Y. N.; Belokon, P. Carta, M. North, *Tetrahedron Lett.* **2005**, *46*, 4483–4486 Belokon, S. Caveda-Cepas, B. Green, N. S. Ikonnikov, V. N. Khrustalev, V. S. Larichev, M. A. Moscalenko, M. North, C. Orizu, V. I. Tararov, M. Tasinazzo, G. I. Timofeeva, L. V. Yashkina, *J. Am. Chem. Soc.* **1999**, *121*, 3968–3973; b) Y. N. Belokon, B. Green, N. S. Ikonnikov, M. North, V. I. Tararov, *Tetrahedron Lett.* **1999**, *40*, 8147–8150.

[7] For a review of the development and applications of this catalyst see: T. R. J. Achard, L. A. Clutterbuck, M. North, *Synlett* **2005**, 1828–1847.

[8] a) Y. Hamashima, D. Sawada, M. Kanai, M. Shibasaki, *J. Am. Chem. Soc.* **1999**, *121*, 2641–2642; b) Y. Hamashima, D. Sawada, H. Nogami, M. Kanai, M. Shibasaki, *Tetrahedron*, **2001**, *57*, 805–814.

[9] For reviews of the applications of catalysts **2** and **4** see: a) H. Gröger, *Chem. Eur. J.* **2001**, *7*, 5246–5251; b) M. Shibasaki, M. Kanai, K. Funabashi, *Chem. Commun.* **2002**, 1989–1999; c) M. Kanai, N. Kato, E. Ichikawa, M. Shibasaki, *Synlett* **2005**, 1491–1508.

[10] a) J. Casas, C. Nájera, J. M. Sansano, J. M. Saá, *Org. Lett.* **2002**, *4*, 2589–2592; b) J. Casas, C. Nájera, J. M. Sansano, J. M. Saá, *Tetrahedron* **2004**, *60*, 10487–10496.

[11] a) Y. Hamashima, M. Kanai, M. Shibasaki, *J. Am. Chem. Soc.* **2000**, *122*, 7412–7413; b) K. Yabu, S. Masumoto, S. Yamasaki, Y. Hamashima, M. Kanai, W. Du, D. P. Curran, M. Shibasaki, *J. Am. Chem. Soc.* **2001**, *123*, 9908–9909; c) Y. Hamashima, M. Kanai, M. Shibasaki, *Tetrahedron Lett.* **2001**, *42*, 691–694; d) K. Yabu, S. Masumoto, M. Kanai, D. P. Curran, M. Shibasaki, *Tetrahedron Lett.* **2002**, *43*, 2923–2926; e) M. Takamura, K. Yabu, T. Nishi, H. Yanagisawa, M. Kanai, M. Shibasaki, *Synlett* **2003**, 353–356; f) S. Masumoto, M. Suzuki, M. Kanai, M. Shibasaki, *Tetrahedron Lett.* **2002**, *43*, 8647–8651; g) S. Masumoto, M. Suzuki, M. Kanai, M. Shibasaki, *Tetrahedron* **2004**, *60*, 10497–10504; h) M. Suzuki, N. Kato, M. Kanai, M. Shibasaki, *Org. Lett.* **2005**, *7*, 2527–2530.

[12] a) Y. N. Belokon, J. Blacker, L. A. Clutterbuck, M. North, *Org. Lett.* **2003**, *5*, 4505–4507; b) J. Casas, A. Baeza, J. M. Sansano, C. Nájera, J. M. Saá, *Tetrahedron: Asymmetry* **2003**, *14*, 197–200; c) Y. N. Belokon, E. Ishibashi, H. Nomura, M. North, *Chem. Commun.* **2006**, 1775–1777; d) A. Baeza, J. Casas, C. Nájera, J. M. Sansano, *J. Org. Chem.* **2006**, *71*, 3837–3848; e) A. Baeza, J. Casas, C. Nájera, J. M. Sansano, J. M. Saá, *Eur. J. Org. Chem.* **2006**, 1949–1958; f) Y. N. Belokon, W. Clegg, R. W. Harrington, E. Ishibashi, H. Nomura M. North, *Tetrahedron* **2007**, *63*, 9724–9740.

[13] a) A. Baeza, J. Casas, C. Nájera, J. M. Sansano, J. M. Saá, *Angew. Chem.* **2003**, *115*, 3251–3254; *Angew. Chem. Int. Ed.* **2003**, *42*, 3143–3146; b) A. Baeza, C. Nájera, J. M. Sansano, J. M. Saá, *Chem. Eur. J.* **2005**, *11*, 3849–3862; c) A. Baeza, C. Nájera, J. M. Sansano, *Eur. J. Org. Chem.* **2007**, 1101–1112.

[14] a) A. Baeza, C. Nájera, J. M. Sansano, J. M. Saá, *Tetrahedron: Asymmetry* **2005**, *16*, 2385–2389; b) S. Lundgren, E. Wingstrand, M. Penhoat, C. Moberg, *J. Am. Chem. Soc.* **2005**, *127*, 11592–11593; c) E. Wingstrand, S. Lundgren, M. Penhoat, C. Moberg, *Pure Appl. Chem.* **2006**, *78*, 409–411; d) S. Lundgren, E. Wingstrand, C. Moberg, *Adv. Synth. Catal.* **2007**, *349*, 364–372.

[15] a) S. S. Kim, S. H. Lee, *Synth. Commun.* **2005**, *35*, 751–759; b) S. S. Kim, S. H. Lee, J. M. Kwak, *Tetrahedron: Asymmetry* **2006**, *17*, 1165–1169; c) S. S. Kim, J. M. Kwak, S. C. George, *Appl. Organomet. Chem.* **2007**, *21*, 809–813.

[16] a) D. A. Nicewicz, C. M. Yates, J. S. Johnson, *Angew. Chem.* **2004**, *116*, 2706–2709; *Angew. Chem. Int. Ed.* **2004**, *43*, 2652–2655; b) F.-X. Chen, H. Zhou, X. Liu, B. Qin, X. Feng, G. Zhang, Y. Jiang, *Chem. Eur. J.* **2004**, *10*, 4790–4797; c) D. A. Nicewicz, C. M. Yates, J. S. Johnson, *J. Org. Chem.* **2004**, *69*, 6548–6555; d) S. S. Kim, D. H. Song, *Eur. J. Org. Chem.* **2005**, 1777–1780; e) S. S. Kim, *Pure Appl. Chem.* **2006**, *78*, 977–983; f) S. S. Kim, J. M. Kwak, *Tetrahedron* **2006**, *62*, 49–53.

[17] I. P. Holmes, H. B. Kagan, *Tetrahedron Lett.* **2000**, *41*, 7457–7460.

[18] a) Y. N. Belokon, M. North, T. Parsons, *Org. Lett.* **2000**, *2*, 1617–1619; b) Y. N. Belokon, B. Green, N. S. Ikonnikov, M. North, T. Parsons, V. I. Tararov, *Tetrahedron* **2001**, *57*, 771–779.

[19] a) S. Hanessian, G. J. Reddy, N. Chahal, *Org. Lett.* **2006**, *8*, 5477–5480; b) G. C. Lloyd-Jones, P. D. Wall, J. L. Slaughter, A. J. Parker, D. P. Laffan, *Tetrahedron* **2006**, *62*, 11402–11412.

[20] Y. N. Belokon, V. I. Maleev, M. North, D. L. Usanov, *Chem. Commun.* **2006**, 4614–4616.

[21] a) Y. N. Belokon, A. V. Gutnov, M. A.; Moskalenko, L. V. Yashkina, D. E. Lesovoy, N. S. Ikonnikov, V. S. Larichev, M. North, *Chem. Commun.* **2002**, 244–245; A. V. Gutnov, M. A.; Moskalenko, L. V. Yashkina, D. E. Lesovoy, N. S. Ikonnikov, V. S. Larichev, M. North, *Chem. Commun.* **2002**, 244–245; b) Y. N. Belokon, P. Carta, A. V. Gutnov, V. Maleev, M. A. Moskalenko, L. V. Yashkina, N. S. Ikonnikov, N. V. Voskoboev, V. N. Khrustalev, M. North, *Helv. Chim. Acta* **2002**, *85*, 3301–3312; c) Y. N. Belokon, P. Carta, M. North, *Lett. Org. Chem.* **2004**, *1*, 81–83; d) Y. N. Belokon, A. J. Blacker, P. Carta, L. A. Clutterbuck, M. North, *Tetrahedron* **2004**, *60*, 10433–10447; e) M. North, A. W. Parkins, A. N. Shariff, *Tetrahedron Lett.* **2004**, *45*, 7625–7627; f) Y. N.; Belokon, P. Carta, M. North, *Tetrahedron Lett.* **2005**, *46*, 4483–4486; g) Y. N. Belokon, A. J. Blacker,

L. A. Clutterbuck, D. Hogg, M. North, C. Reeve, *Eur. J. Org. Chem.* **2006**, 4609–4617.

[22] a) C. Baleizão, B. Gigante, H. Garcia, A. Corma, *J. Catal.* **2003**, *215*, 199–207; b) C. Baleizão, B. Gigante, D. Das, M. Alvaro, H. Garcia, A. Corma, *Chem. Commun.* **2003**, 1860–1861; c) W. Huang, Y. Song, C. Bai, G. Cao, Z. Zheng, *Tetrahedron Lett.* **2004**, *45*, 4763–4767; d) C. Baleizão, B. Gigante, H. Garcia, A. Corma, *Tetrahedron* **2004**, *60*, 10461–10468; e) W. Huang, Y. Song, J. Wang, G. Cao, Z. Zheng, *Tetrahedron* **2004**, *60*, 10469–10477; f) C. Baleizão, B. Gigante, H. Garcia, A. Corma, *J. Catal.* **2004**, *221*, 77–84; g) N. H. Khan, S. Agrawal, R. I. Kureshy, S. H. R. Abdi, V. J. Mayani, R. V. Jasra, *Tetrahedron: Asymmetry* **2006**, *17*, 2659–2666; S. H. R. Abdi, V. J. Mayani, R. V. Jasra, *Tetrahedron: Asymmetry* **2006**, *17*, 2659–2666; h) N. H. Khan, S. Agrawal, R. I. Kureshy, S. H. R. Abdi, V. J. Mayani, R. V. Jasra, *Eur. J. Org. Chem.* **2006**, 3175–3180; i) N. H. Khan, S. Agrawal, R. I. Kureshy, S. H. R. Abdi, V. J. Mayani, R. V. Jasra, *J. Mol. Catal. A* **2007**, *264*, 140–145.

[23] For a related recent study on the mechanism of asymmetric cyanohydrin synthesis using a non-metallic catalyst see: S. J. Zuend, E. N. Jacobsen, *J. Am. Chem. Soc.* **2007**, *129*, 15872–15883.

[24] K. Oyaizu, E. L. Dewi, E. Tsuchida, *Inorg. Chem.* **2003**, *42*, 1070–1075.

[25] K. Nakajima, K. Kojima, M. Kojima, J. Fujita, *Bull. Chem. Soc. Jpn.* **1990**, *63*, 2620–2630.

[26] S. Norsikian, I. Holmes, F. Lagasse, H. B. Kagan, *Tetrahedron Lett.* **2002**, *43*, 5715–5717.

[27] a) Y. N. Belokon, B. Green, N. S. Ikonnikov, V. S. Larichev, B. V. Lokshin, M. A. Moscalenko, M. North, C. Orizu, A. S. Peregudov, G. I. Timofeeva, *Eur. J. Org. Chem.* **2000**, 2655–2661; b) Y. N. Belokon, W. Clegg, R. W. Harrington, C. Young, M. North, *Tetrahedron* **2007**, *63*, 5287–5299.

[28] Data included in the supporting information. This includes: All of the kinetic plots used to derive the rate equation, construct Figure 3, and generate the data in Table 2 and Table 5. Kinetic plots for reactions using complexes **5** and **6c–g** under argon and oxygen atmospheres. Kinetic plots for control reactions involving 6-methoxynaphth-2-aldehyde. The high-resolution positive ion mode electrospray mass spectra of complexes **5, 6a–g**, and **8a–m**. ^{1}H NMR spectra for complexes **5, 6a–g**, and **8a–m**. Cyclic voltamograms for complexes **6b–e**,**g**. UV spectra for VO(salen) and complexes **6e**,**g**. Details of all chemicals and equipment used. Synthetic procedures and characterizing data for complexes **5, 6a–g**, and **8a–m**. Characterizing data for cyanohydrin trimethylsilyl ethers **20a–m**. Details of the detection of benzoic acid.

[29] N. F. Choudhary, P. B. Hitchcock, G. J. Leigh, *Inorg. Chim. Acta* **2000**, *310*, 10–20.

[30] A. Horn Jr. , C. A. L. Filgueiras, J. L. Wardell, M. H. Herbst, N. V. Vugman, P. S. Santos, J. G. S. Lopes, R. A. Howie, *Inorg. Chim. Acta* **2004**, *357*, 14240–14246.

[31] a) M. Tsuchimoto, E. Yasuda, S. Ohba, *Chem. Lett.* **2000**, 562–563; b) P. Hald, A. Hazell, T. R. Jensen, H. F. Jensen, J.-E. Jørgensen, *Acta Crystallogr. Sect. E* **2001**, *57*, m310–m312; c) A. Hazell, P. Lund, A. Saugbjerg, *Acta Crystallogr. Sect. C* **2001**, *57*, 257–259.

[32] a) M. Mazzanti, S. Gambarotta, C. Floriani, A. Chiesi-Cilla, C. Guastini, *Inorg. Chem.* **1986**, *25*, 2308–2314; b) D. G. McCollum, G. P. A. Yap, L. Liable-Sands, A. L. Rheingold, B. Bosnich, *Inorg. Chem.* **1997**, *36*, 2230–2235; G. P. A. Yap, L. Liable-Sands, A. L. Rheingold, B. Bosnich, *Inorg. Chem.* **1997**, *36*, 2230–2235; c) H. Schmidt, D. Rehder, *Inorg. Chim. Acta* **1998**, *267*, 229–238.

[33] K. Mai, G. Patil, *J. Org. Chem.* **1986**, *51*, 3545–3548.

[34] For oxidation of alcohols see: A. T. Radosevich, C. Musich, F. D. Toste, *J. Am. Chem. Soc.* **2005**, *127*, 1090–1091.

[35] For oxidation of sulfides see: a) K. Nakajima, M. Kojima, J. Fujita, *Chem. Lett.* **1986**, 1483–1486; b) H. Schmidt, M. Bashirpoor, D. Rehder, *J. Chem. Soc. Dalton Trans.* **1996**, 3865–3870.

[36] For oxidation of phenols see: P. P. Reddy, C.-Y. Chu, D.-R. Hwang, S.-K. Wang, B.-J. Uang, *Coord. Chem. Rev.* **2003**, *237*, 257–269.

[37] For previous reports of the formation of oligomeric oxovanadium-(salen) complexes containing both vanadium(IV) and vanadium(V)

ions see: a) A. Hills, D. L. Hughes, G. J. Leigh, J. R. Sanders, *J. Chem. Soc. Dalton Trans.* **1991**, 61–64; b) D. L. Hughes, U. Kleinkes, G. J. Leigh, M. Maiwald, J. R. Sanders, C. Sudbrake, *J. Chem. Soc. Dalton Trans.* **1994**, 2457–2466; c) K. Yamamoto, K. Oyaizu, E. Tsuchida, *J. Am. Chem. Soc.* **1996**, *118*, 12665–12672; d) K. Oyaizu, K. Yamamoto, K. Yoneda, E. Tsuchida, *Inorg. Chem.* **1996**, *35*, 6634–6635; e) N. F. Choudhary, N. G. Connelly, P. B. Hitchcock, G. J. Leigh, *J. Chem. Soc. Dalton Trans.* **1999**, 4437–4446; f) Y. N. Belokon, W. Clegg, R. W. Harrington, M. North, C. Young, *Inorg. Chem.* **2008**, *47*, 3801–3814.

[38] The order with respect to the catalyst (*x*) will itself be temperature dependent, reflecting the temperature dependence of the equilibrium between mononuclear and polynuclear forms of complexes **1**, **5**, and **6**.[27a] However, the goodness of fit of the data in Figure 3 to straight lines suggest that over the temperature range used for this study, the variation in *x* is negligible, so the values determined at 273 K were used.

[39] A. Williams, *Free Energy Relationships in Organic and Bio-organic Chemistry*, Royal Society of Chemistry, London, **2003**.

[40] a) J. A. Bonadies, W. M. Butler, V. L. Pecoraro, C. J. Carrano, *Inorg. Chem.* **1987**, *26*, 1218–1222; b) E. Tsuchida, K. Oyaizu, E. L. Dewi, T. Imai, F. C. Anson, *Inorg. Chem.* **1999**, *38*, 3704–3708.

[41] G. Shan, B. D. Hammock, *Anal. Biochem.* **2001**, *299*, 54–62.

[42] For the use of the same aldehyde as a fluorescent probe of antibody catalyzed retro-aldol reactions see: B. List, C. F. Barbas(III), R. A. Lerner, *Proc. Natl. Acad. Sci. USA* **1998**, *95*, 15351–15355.

[43] a) G. Hoshina, M. Tsuchimoto, S. Ohba, K. Nakajima, H. Uekusa, Y. Ohashi, H. Ishida, M. Kojima, *Inorg. Chem.* **1998**, *37*, 142–145; b) Z. Liu, F. C. Anson, *Inorg. Chem.* **2001**, *40*, 1329–1333; c) D. M. Boghaei, S. Mohebi, *J. Mol. Cat. A* **2002**, *179*, 41–51; d) E. Tsuchida, K. Oyaizu, *Coord. Chem. Rev.* **2003**, *237*, 213–228.

[44] A related mechanism has been proposed to account for catalysis by mononuclear Schiff base complexes of titanium: M. Hayashi, Y. Miyamoto, T. Inoue, N. Oguni, *J. Org. Chem.* **1993**, *58*, 1515–1523.

[45] Benzoic acid was detected in the reaction mixture by high resolution electrospray mass spectrometry. This data is included in the Supporting Information.

[46] Structure **16** is shown in the isonitrile form for clarity, but is expected to exist as an equilibrium mixture of nitrile and isonitrile forms.

[47] For a detailed analysis of the configurations adopted by salen ligands in octahedral complexes see reference [27b]. See also: a) A. M. Sargeson, G. H. Searle *Inorg. Chem.* **1965**, *4*, 45–52; b) U. Knof, A. von Zelewsky, *Angew. Chem.* **1999**, *111*, 312–333; *Angew. Chem. Int. Ed.* **1999**, *38*, 302–322; c) V. I. Tararov, V. S. Larichev, M. A. Moscalenko, L. V. Yashkina, V. N. Khrustalev, M. Y. Antipin, A. Börner, Y. N. Belokon, *Enantiomer* **2000**, *5*, 169–173.

[48] For a review of asymmetric catalysis by (salen)metal complexes in which the salen ligand adopts the *cis*-β configuration see: T. Katsuki, *Chem. Soc. Rev.* **2004**, *33*, 437–444.

[49] Metalloacetal units are well precedented. For crystal structures see: a) F. Ebina, A. Ouchi, Y. Yoshino, S. Sato, Y. Saito, *Acta Crystallogr. Sect. B* **1977**, *33*, 3252–3253; b) F. Ebina, A. Ouchi, Y. Yoshino, S. Sato, Y. Saito, *Acta Crystallogr. Sect. B* **1978**, *34*, 1512–1515; c) P. Bradford, R. C. Hynes, N. C. Payne, C. J. Willis, *J. Am. Chem. Soc.* **1990**, *112*, 2647–2654; d) C. E. Housmekerides, R. S. Pilato, G. L. Geoffroy, A. L. Rheingold, *J. Chem. Soc. Chem. Commun.* **1991**, 563–566; e) R. C. Hynes, C. J. Willis, N. C. Payne, *Acta Crystallogr. Sect. C* **1992**, *48*, 42–45; f) C. E. Housmekerides, D. L. Ramage, C. M. Kretz, J. T. Shontz, R. S. Pilato, G. L. Geoffroy, A. L. Rheingold, B. S. Haggerty, *Inorg. Chem.* **1992**, *31*, 4453–4468; g) M. Parvez, S. Ali, T. M. Masood, M. Mazhar, M. Danish, *Acta Crystallogrr. Sect. C* **1997**, *53*, 1211–1213; h) M. J. Scott, S. J. Lippard, *Organometallics* **1998**, *17*, 466–474; i) A. V. Gushchin, R. I. Usyatinsky, G. K. Fukin, V. A. Dodonov, L. N. Zakharov, *Main Group Chem.* **1998**, *2*, 187–190.

[50] For previous examples of octahedral, monometallic salen complexes in which the salen ligand adopts a *cis*-β configuration due to the presence of an additional bidentate ligand see: a) N. A. Bailey, B. M. Higson, E. D. McKenzie, *J. Chem. Soc. Dalton Trans.* **1972**, 503–

507; b) M. Calligaris, G. Manzini, G. Nardin, L. Randaccio, *J. Chem. Soc. Dalton Trans.* **1972**, 543–546; c) M. Gullotti, A. Pasini, G. M. Zanderighi, G. Ciani, A. Sironi, *J. Chem. Soc. Dalton Trans.* **1981**, 902–908; d) R. B. Lauffer, R. H. Heistand(II), L. Que(Junior), *Inorg. Chem.* **1983**, *22*, 50–55; e) F. Lloret, M. Julve, M. Mollar, I. Castro, J. Latorre, J. Faus, X. Solans, I. Morgenstern-Badarau, *J. Chem. Soc. Dalton Trans.* **1989**, 729–738; f) M. J. Maroney, R. O. Day, T. Psyris, L. M. Fleury, J. P. Whitehead, *Inorg. Chem.* **1989**, *28*, 173–175; g) I. Malfant, I. Morgenstern-Badarau, M. Philoche-Levi-salles, F. Lloret, *J. Chem. Soc. Chem. Commun.* **1990**, 1338–1340; h) M. Ohba, H. Tamaki, N. Matsumoto, H. Okawa, *Inorg. Chem.* **1993**, *32*, 5385–5390; i) K. M. Carroll, J. Schwartz, D. M. Ho, *Inorg. Chem.* **1994**, *33*, 2707–2708; j) V. Vergopoulos, S. Jantzen, D. Rode-wald, D. Rehder, *J. Chem. Soc. Chem. Commun.* **1995**, 377–378; k) D. Agustin, G. Rima, H. Gornitzka, J. Barrau, *J. Organomet. Chem.* **1999**, *592*, 1–10; l) W. J. Evans, C. H. Fujimoto, J. W. Ziller, *Polyhedron* **2002**, *21*, 1683–1688.

[51] a) F.-X. Chen, X. Feng, *Synlett* **2005**, 892–899; b) I. V. P. Raj, G. Sur-yavanshi, A. Sudalai, *Tetrahedron Lett.* **2007**, *48*, 7211–7214.

[52] The reaction carried out in the presence of 0.01 mol% of tetrabutyl-ammonium chloride showed a very good fit to both first- and second-order kinetics ($R^2 = 0.99$ and 1.00) respectively, but is ana-lyzed according to first order kinetics to allow the rate to be com-pared with other concentrations of tetrabutylammonium chloride.

[53] F. H. Allen, *Acta Crystallogr. Sect. B* **2002**, *58*, 380–388.

[54] a) S. A. Fairhurst, D. L. Hughes, G. J. Leigh, J. R. Sanders, J. Weis-ner, *J. Chem. Soc. Dalton Trans.* **1994**, 2591–2598; b) K. Oyaizu, E. Tsuchida, *J. Am. Chem. Soc.* **2003**, *125*, 5630–5631.

[55] M. Tsuchimoto, S. Ohba, *Acta Crystallogr. Sect. C* **1999**, *55*, IUC9900008.

[56] The dinuclear catalytic cycle shown in Scheme 6 can easily be modi-fied to accommodate catalysis by any oligomeric species of general structure $[V^{IV}(salen)=O]_n[V^V(salen)=O]X$ and there is ample litera-ture precedent for the formation of such oligomers. See reference [37].

[57] J. Brussee, E. C. Roos, A. van der Gen, *Tetrahedron Lett.* **1988**, *29*, 4485–4488.

[58] F. Effenberger, J. Eichhorn, *Tetrahedron: Asymmetry* **1997**, *8*, 469–476.